Large scale collective modeling the final "Freeze Out" stages of energetic heavy ion reactions and calculation of single particle measurables from these models

Ágnes Nyíri

Thesis submitted in partial fullfillment of the requirements for the degree of Philosophiae Doctor

July 2005

Department of Physics and Technology
University of Bergen

Bergen, Norway 2005

Acknowledgments

There are several people who absolutely deserve my honest gratitude for their contribution one way or another to the work compiled in this thesis.

First of all, I would like to thank my supervisor, Prof. László Pál Csernai for his guidance and assistance. His knowledge and insight into a wide range of topics never cease to amaze me, and provided me with invaluable help during my work. I am indebted to him for introducing me into the field of heavy ion collisions.

I am grateful to my colleagues and friends at the Department of Physics, University of Bergen, for maintaining a good environment for both research and friendship. In particular, I would like to thank Etele Molnár, my office mate and almost-neighbour, for stimulating and sometimes rather fiery discussions. I highly appreciate his cheerful company, which made the days at work more enjoyable. Matthias Richter, Hongyan Yang and Sven Zschocke deserve special thanks for the nice conversations, which helped me to overcome my rather gloomy mood many times during the finalization of the thesis.

I am deeply grateful to Halvor Møll Nilsen for his careful reading of the manuscript and for the enlightening questions and comments on the thesis. I wish to thank him for his patience and invaluable support.

I wish to express my deepest gratitude for having a supportive family. I am specially thankful to my parents and my sister for the encouragement, which gave me inspiration for going on even in the hardest moments of the work. I am also indebted to Anne Ruth and Rune Nilsen for their kindness, constant support and care.

Ágnes Nyíri
Bergen, July 2005

List of papers

During my PhD studies I was co-author of 13 scientific papers. Ten of these have already been published or accepted for publication in refereed international journals and conference proceedings. Two of our papers have been submitted to *Physical Review* **C**, and are under consideration. Our latest article is now ready for submission. A list of these papers is given below. My two earlier publications are also listed, however, these are not related directly to my PhD project.
This thesis is based on eight papers, which can be found in appendix C.

Papers included in the thesis

Papers on Modified Boltzmann Transport Equation

C.1 *Modified Boltzmann Transport Equation*
V.K. Magas, L.P. Csernai, E. Molnár, Á. Nyíri and K. Tamosiunas
Nucl. Phys. **A 749** (2005) 202, (hep-ph/0502185).

C.2 *Modified Boltzmann Transport Equation and Freeze Out*
L.P. Csernai, V.K. Magas, E. Molnár, Á. Nyíri and K. Tamosiunas
Eur. Phys. J. **A 25** (2005) 65, (hep-ph/0505228).

C.3 *Freeze Out and the Boltzmann Transport Equation*
L.P. Csernai, V.K. Magas, E. Molnár, Á. Nyíri and K. Tamosiunas
to be submitted to *Phys. Rev.* **C** *Rap. Comm.* (revised version of hep-ph/0406082).

Papers on covariant freeze out description through a finite layer

C.4 *Covariant Description of Kinetic Freeze Out Through a Finite Space-like Layer*
E. Molnár, L.P. Csernai, V.K. Magas, Á. Nyíri and K. Tamosiunas
Submitted to *Phys. Rev.* **C**, (hep-ph/0503047).

C.5 *Covariant Description of Kinetic Freeze Out Through a Finite Time-like Layer*
E. Molnár, L.P. Csernai, V.K. Magas, Zs.I. Lázár, Á. Nyíri and K. Tamosiunas
Submitted to *Phys. Rev.* **C**, (hep-ph/0503048).

Papers on collective flow in heavy ion collisions

C.6 *The 3rd Flow Component as a QGP Signal*
L.P. Csernai, A. Anderlik, Cs. Anderlik, V.K. Magas, E. Molnár, Á. Nyíri, D. Röhrich and K. Tamosiunas
Acta Phys. Hung. **A**, in press (2005), (hep-ph/0405277).

C.7 *Collective Phenomena in Heavy Ion Collisions*
Á. Nyíri and L.P. Csernai
Acta Phys. Hung. **A**, in press (2005).

C.8 *Collective Phenomena in Heavy Ion Collisions*
Á. Nyíri, L.P. Csernai, E. Molnár and K. Tamosiunas
J. Phys. **G 31** (2005) 1045.

Papers not included in the thesis

1. *Modeling of Boltzmann Transport Equation for Freeze Out*
   K. Tamosiunas, L.P. Csernai, V.K. Magas, E. Molnár, Á. Nyíri
   J. Phys. **G 31** (2005) 1001.

2. *Hydrodynamics: Overview*
   L.P. Csernai, E. Molnár, Á. Nyíri and K. Tamosiunas
   J. Phys. **G 31** (2005) 951.

3. *Phase Transitions in High Energy Heavy Ion Collisions*
   L.P. Csernai, A. Anderlik, Cs. Anderlik, A. Keranen, V.K. Magas, J. Manninen, E. Molnár, Á. Nyíri, B.R. Schlei, D.D.Strottman and K. Tamosiunas
   Proceedings of NATO ASI on *Structure and Dynamics of Elementary Matter* (2004) p. 127, ISBN 1-4020-2445-2, edited by W. Greiner, M.G. Itkis, J. Reinhardt and M. Cem Guclu, (hep-ph/0401005).

4. *Multi Module Modeling of Heavy Ion Reactions and the 3rd Flow Component*
   L.P. Csernai, A. Anderlik, Cs. Anderlik, V.K. Magas, E. Molnár, Á. Nyíri, D. Röhrich and K. Tamosiunas

AIP Conference Proceedings Vol. 739 (2004) p. 330, ISBN 0 7354 0223 X, edited by E. Ferreira and T. Kodama, (hep-ph/0408183).

5. *Canceling Jüttner Distributions for Space-like Freeze Out*
   K. Tamosiunas, L.P. Csernai, J. Manninen, E. Molnár and Á. Nyíri
   AIP Conference Proceedings Vol. 739 (2004) p. 652, ISBN 0 7354 0223 X, edited by E. Ferreira and T. Kodama.

Earlier papers not related to the thesis

1. *Quark–Gluon Plasma Tomography by Vector Mesons*
   I. Lovas, L.P. Csernai, Á. Nyíri and Zs. Schram
   Heavy Ion Physics **13** (2001) No. 4, 289.

2. *Neutron Stars with and without Strange Matter Core*
   Á. Nyíri
   J. Phys. **G 28** (2002) 2073.

Contents

List of Figures

Chapter 1

Introduction

"If it were possible to experiment with neutrons or protons of energies above hundred million volts, several charged or uncharged particles would eventually leave the nucleus or as a result of the encounter; with particles of energies about a thousand of million of volts, we must even be prepared for the collision to lead to an explosion of the whole nucleus."
Niels Bohr, Nature 137 (1936) 351.

1.1 Quark-gluon plasma and heavy ion collisions

The high density and high temperature behaviour of nuclear matter is still quite unknown and has led to speculations about the appearance of new phases. Under conditions of high density and temperature, hadronic matter is expected to undergo a phase transition to deconfined quark matter, in which quarks – instead of being bound in more complex particles such as protons and neutrons – are liberated to roam freely forming the so-called *Quark-Gluon Plasma* (QGP). Already about 30 years ago it was predicted that these conditions may be achieved for a brief moment in energetic heavy ion collisions [1].

Experimental attempts to create the QGP in the laboratory and measure its properties have been carried out for more than 20 years by studying collisions of heavy nuclei and analyzing the fragments and produced particles emerging from such collisions.

The aim of heavy ion experiments is to create immensely high energy densities, which can break down the forces confining quarks inside more complex particles. During the last two decades, center of mass energies per pair of colliding nucleons have risen steadily from the $\sqrt{s_{NN}} \approx 1\,\mathrm{GeV}$ domain of the BEVALAC at LBNL, to energies of $\sqrt{s_{NN}} = 5\,\mathrm{GeV}$ at the AGS at BNL, and

to $\sqrt{s_{NN}} = 17\,\text{GeV}$ at the Super Proton Synchrotron (SPS) at CERN. No decisive evidence of QGP formation was found in the experiments at those energies, although a number of signals suggesting the formation of a *new state of matter* were found at the SPS [2, 3].

In this experiment a very high energy beam of lead ions (33 TeV) was accelerated and crashed into targets inside seven different experimental detectors. The collisions created temperatures over 100 thousand times as hot as the center of the Sun, and energy densities twenty times that of the ordinary nuclear matter.

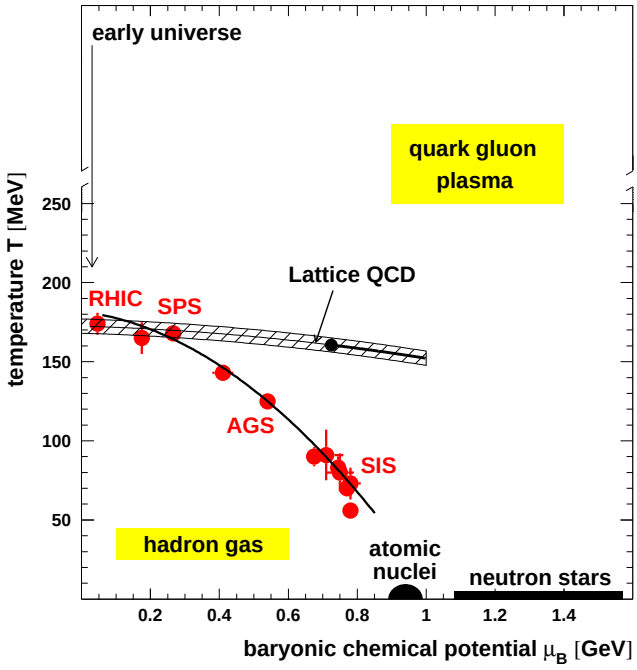

Figure 1.1: QCD phase diagram summarizing the present understanding about the structure of nuclear matter at different densities and temperatures. The points illustrates the results achieved by the different ultra-relativistic collider experiments, and the dashed line represents the lattice QCD calculations.

Actually, this exotic phase of matter is not new to the universe, just to human eyes. It is thought to have existed in the first few microseconds after the Big Bang at the dawn of the universe, when the temperature was still sufficiently high, and it is likely to appear in the Nature even now. A very high density – and comparatively low temperature – environment exists in the interior of neutron stars, which may actually contain significant amounts of quark matter in their cores. The possibility of different phase transitions taking place in the superdense interior of neutron stars has also been the

target of considerable interest during the last few decades (see [4–6] and references therein).

The present experimental and theoretical knowledge about the different phases of nuclear matter can be summarized in a QCD phase diagram, which is shown in figure 1.1. The results achieved by the relativistic collider experiments (SIS, AGS, SPS and RHIC) are indicated in the figure. Recent lattice QCD results are also shown. According to the lattice QCD calculations [7, 8], the phase transition takes place in a narrow temperature interval around $T_c \sim$170 MeV. The results show a slight decrease of the critical temperature, T_c, with increasing baryonic chemical potential, μ_B. However, there is no reliable calculation for values of μ_B higher than the chemical potential of normal nuclear matter. One can see that the experiments with lower energies, such as SIS and AGS, do not reach the critical zone, while RHIC and SPS do. Thus, QGP might have been formed in the two latter experiments.

1.2 Motivation for the work

There are still many open questions regarding the properties and behaviour of fundamental matter under extreme conditions, therefore, the research for solving the puzzles of matter is still going on. New, large scale experiments have been started at the Relativistic Heavy Ion Collider (RHIC) at Brookhaven National Laboratory in the US, and the next research instrument in Europe's particle physics armory, the Large Hadron Collider (LHC) in CERN, is under construction, and will start operating in 2007.

RHIC started regular beam operations in the summer of year 2000 with a short run colliding gold (Au) nuclei at energies of $\sqrt{s_{NN}} = 130$ GeV. The first full run at the top energy ($\sqrt{s_{NN}} = 200$ GeV) took place in the fall/winter of 2001/2002. The third RHIC run during the winter/spring of 2003 focused on d+Au and p+p reactions. In 2004, a long high luminosity Au+Au run at $\sqrt{s_{NN}} = 200$ GeV and a short run at $\sqrt{s_{NN}} = 62.4$ GeV were completed. The collected data from the most recent runs are currently being analyzed and only a few early results are thus available at the time of writing of this thesis. The large number of articles already produced by the four experiments at RHIC may be found on their respective homepages [9].

However, the experiments alone are not able to provide us with new knowledge on the properties of the new state of matter formed in the collisions. Quark-gluon plasma is created at the beginning of the heavy ion collision and lasts only for a very short time. Thus, by the end of the reaction all the QGP has vanished, and the experimental instruments detect only an intense shower of different particles with different momenta. The huge amount of information, which all these detected particles carry might help us to determine the collision mechanism of heavy ion reactions and gain

the desired knowledge on the matter, where these particles are coming from. This is the point, where the theoretical work gets the main role in further analysis. In order to understand what happened in the collision before all those particles were created, one needs a complete theoretical description of the heavy ion reaction.

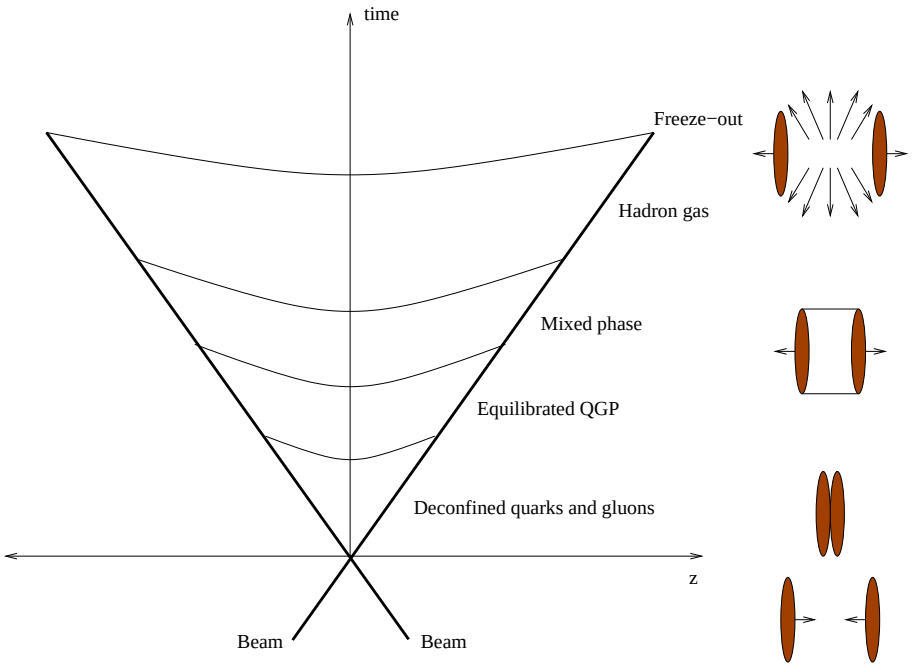

Figure 1.2: The Bjorken space-time scenario for a heavy ion collision. The two colliding nuclei resemble two flat discs because of the Lorentz contraction in the laboratory frame.

To illustrate the theoretical challenge, which one is confronted with while modeling energetic heavy ion collisions, let us give a very short and highly simplified introduction into the dynamics of heavy ion reactions.

First, two highly Lorentz contracted nuclei approach one another. The two ions collide, smashing into one another and then passing through each other. Some of the energy they had before the collision is transformed into intense heat and new particles. If conditions are right, the protons and neutrons dissolve into their constituents for a brief time and deconfined quarks and gluons are created. This matter constitutes the *pre-equilibrium phase*. After a certain formation time, which is likely to be 0.5 to 2 fm/c, the system is believed to reach local thermal equilibrium, provided that there are enough interactions among the constituents. This equilibrated state is the *quark-gluon plasma* phase.

As the system expands, the equilibrated plasma of deconfined quarks and

gluons quickly cools down to the temperature, where a phase transition into a hadron gas takes place. Depending on the type of the transition, the system may spend some time in a mixed phase where the QGP coexists with the hadron gas. Finally, the size of the system becomes larger than the mean free path of hadrons, they undergo a *freeze out* and stream freely towards the detectors. This freeze out process is most usually treated as a sudden freeze out, implying that at a given instant in the space-time all constituents within the fluid become independent, and final interactions and collisions are becoming negligible. A schematic view of the dynamics is shown in figure 1.2, which is based on Bjorken's scaling hydrodynamical model [10].

So far none of the existing theoretical models can claim to describe all the stages of the ultra-relativistic heavy ion collisions. Our goal has been to develop a complete combined model and gain information on the statistical properties of the quark-gluon plasma, primarily of the equation of state, by using this model. Any realistic model must include several "modules" to describe the different stages of the reaction. The locally equilibrated state of QGP is formed only in the intermediate stages of the reaction. The initial and final stages are far out of equilibrium, difficult to model, but very important also if we want to describe the whole reaction accurately and in all details comparable to the experimental results.

1.3 Multi Module Model

Models of Computational Fluid Dynamics (CFD) are widely used to describe heavy ion collisions. Their advantage is that one can vary flexibly the equation of state of the matter and test its consequences on the reaction dynamics and the outcome. This makes the fluid dynamical model a very powerful tool to study possible phase transitions in heavy ion collisions, such as the liquid-gas or the quark-gluon plasma phase transition. In energetic collisions of large heavy ions, especially if a QGP is formed in the collision, one-fluid dynamics is a valid and good description for the intermediate stages of the reaction. On the other hand, the initial and final, freeze out, stages of the reaction are outside the domain of applicability of the fluid dynamical model.

The realistic and detailed description of an energetic heavy ion reaction requires a *Multi Module Model* [12]. Such a model should contain at least three modules for the three main stages of the reaction – initial, middle and freeze out processes – where the different stages of the reaction are each described by suitable theoretical approaches. Furthermore, these modules should be coupled to each other correctly: on the interface, which is a three dimensional hypersurface in space-time, all conservation laws should be satisfied, and entropy should not decrease. These matching conditions have been worked out and studied at the freeze out hypersurface [11–17]. Lots of work

has already been done by our group to build such a Multi Module Model, but further development is necessary to bring this task to completion.

Detailed calculations of the initial state using the *Effective String Rope model* [12, 18, 19] have been developed by our collaborator, Volodymyr Magas. This model is based on earlier Coherent Yang-Mills field theoretical models and introduces effective string tension, based on Monte-Carlo string cascade and parton cascade model results. The model has been improved recently and is now applicable to RHIC and LHC energies. This is the first module of our Multi Module Model and provides us with all the data, which serve as input to the next module describing the middle stages of the collision.

The intermediate stages are described by a high resolution *Computational Fluid Dynamical model* with QGP equation of state. The code uses the particle-in-cell (PIC) method [20, 21] to solve the equations of relativistic fluid dynamics numerically. It was originally written for lower energies, and earlier versions of the code have been applied for several fluid dynamical calculations during the last two decades [22]. The code has been recently improved for ultra-relativistic energies, and it is stable enough to run till late times. The author of this thesis has taken part actively in upgrading this module.

The final, so-called *Freeze Out Module* is particularly important, because it describes the observables, which are then compared to the experimental results. The results from the second module – the fluid dynamical model – are used as input to the last module, which models the freeze out and hadronization processes, and allows the evaluation of measurables. The first challenge is the identification of the *Freeze Out Hypersurface* (FOHS) by employing some freeze out (FO) criteria, e.g. T_{FO}. Afterwards, the measurables can be evaluated based on the identified surface. We have already developed a code to identify the FOHS, which is made of millions of fluid elements. We can view the time development of this surface as a movie and we see that at the late stages fluctuations start to dominate the evolution, clusters are getting formed and then decay. Thus, work must still be done on the FOHS model to avoid inaccuracies in further calculations.

In this thesis we will primarily focus on the freeze out problem and calculation of an important measurable, the anisotropic flow, as the major original achievements of this PhD project are related to these two issues of the heavy ion collision modeling.

1.4 Structure of the thesis

This thesis is based on scientific publications, which are presented in appendix C. Since the presentation of background information in scientific papers is rather limited, we included two chapters and two extra appendices

in the thesis, in order to make it more understandable how these papers contribute to better knowledge about the topics in question. Furthermore, the additional parts may help readers with less experience in the rather special topics and terminology of the papers to understand the main message of the thesis.

The thesis is organized as follows: In chapter 2 we will discuss the freeze out problem starting with a short introduction into the general aspects of the freeze out process. Afterwards, we will give a rather brief overview of the kinetic freeze out models which were developed prior to this PhD project and served as a basis of our model. In our project, we have made several improvements on the existing kinetic freeze out models by adding new elements to them, which may contribute to a more realistic description of the freeze out process. In chapter 2 these new achievements will also be presented, although very briefly, since detailed description of them can be found in the attached papers. The second main subject of our investigation has been the collective flow in heavy ion collisions. Chapter 3 will focus on this very important observable. After summarizing the observables, which were suggested as possible probes of the formation of quark-gluon plasma, we will discuss the importance and methods of anisotropic flow studies in more details, both from theoretical and experimental point of view. We will also give a somewhat extended overview of the techniques of flow analysis in experiments. This is a rather important part of chapter 3, since some of our results are closely related to these techniques, and in the published papers, which contain these results, we could present only a very limited amount of information on the experimental methods. After describing the experimental aspects of flow analysis, we will finally present our original results achieved in this topic.

Then, a summary of the work and conclusions will be given in chapter 4, followed by a brief outlook suggesting some possible improvements, which may be done in the future.

In appendix A the notations and formalism of relativistic kinetic theory and relativistic fluid dynamics are briefly summarized. appendix B contains original derivations of mathematical formulae applied in our flow analysis.

Eight of our scientific papers written during this PhD project are collected in appendix C. Our other published works [23–27], are less relevant for this thesis and are not included.

Finally, a list of the acronyms which were used in the thesis is given in appendix D.

1.5 To the Reader

This thesis has been written in order to complete the requirements for the degree of Philosophiae Doctor in Physics.

It is assumed that the reader is familiar with the elements of quantum and field theories, equilibrium and non-equilibrium statistical physics and the theory of special relativity.

Our project was targeting studies of fundamental matter under extreme conditions by means of high energy heavy ion reactions. Our tool was the so-called Multi Module Model, which describes all of the different stages of heavy ion collisions. In this thesis we did not attempt to give a full description neither of the theory nor the Model. The theory of strongly interacting matter is not presented here in details, because one needs advanced knowledge in Quantum Chromo-Dynamics (QCD) in order to understand its aspects. Meanwhile, details of the first two modules of the Multi Module Model have already been presented elsewhere [12]. Here we will present only the new developments made on the earlier version of the Model during this PhD project.

However, we tried to collect and cite numerous papers and other written works connected to the subject, thus, the interested reader can gain deeper understanding with their help. Here we would like to mention that this thesis has been written at a level to satisfy the interest of other doctoral and maybe master students, although some background education in heavy ion physics and kinetic theory is necessary in order to understand the terminology we use. Because the presentation of the work is rather dense and based on scientific papers, and we are going to describe only very specific aspects of heavy ion collision modeling, therefore, the thesis can be recommended mostly to those who have already been working in this field for a while.

Nevertheless, we do hope that the introductory part to the papers is understandable to all who has some basic background in physics, so they can get an impression on the importance and the main ideas of the modeling of heavy ion collisions.

Chapter 2

The Freeze Out problem

Freeze Out (FO) is a term referring to the last stage of the heavy ion collision, when the particles do not interact anymore and they stream freely towards the detectors. It is a demanding theoretical task to calculate the evolution backward and to extrapolate the initial conditions from the post FO distributions. There are two types of FO discussed in the literature - chemical FO, which fixes the abundances of different hadronic species, and thermal FO, which fixes the momentum distributions for all the species. We simplify our investigation assuming that these two types of freeze out happen at the same time.

The description of the final stages of a heavy ion collision is still problematic and not completely understood. Ever since Landau's Fluid Dynamical model [28] the problem of freeze out is vital to predict measurables. Up to recently the Cooper-Frye formalism [29] was the most widely used method for this purpose. Of course, one has to make sure that energy-momentum and all charges are conserved by choosing post freeze out parameters adequately and that "negative contributions" do not appear when we evaluate the measurables. These two requirements were not considered and were not satisfied by the original Cooper-Frye publication in 1974. In the last years several papers discussed these subjects and provided principle solutions and demonstrated these in simplified models [13–17, 30–35].

Our aim is to work out and demonstrate a freeze out model, which can be applied for realistic reaction models with several millions of elements of the FO hypersurface.

Conservation laws can be satisfied using the relativistic Rankine-Hugoniot or Taub relations [39, 40] if the post FO state is in local thermodynamical equilibrium. Unfortunately, kinetic FO models indicate that the post FO matter is *never* in local equilibrium, so for accurate results, conservation laws have to be evaluated based on the actual post FO matter properties. The use of ideal gas phase space distribution is just a first approximation, and

even this has to be modified to avoid negative contributions by introducing a "cut", first proposed by Bugaev in 1996 [41]. The real, calculated post FO distribution is even more complicated but some analytic approximations do exist. A short summary of these approximated distributions will be given in section 2.2.

In this chapter we will point out the problems one may run into while describing the freeze out process. We will also give a very brief overview of the kinetic FO models. The detailed mathematical and numerical description of the models, which had already existed when this PhD project started can be found in [13–17]. Based on these earlier results, we have introduced new ideas and improved the kinetic FO model by adding new elements to it, which made the description of the process more realistic. In the following sections we will briefly demonstrate these improvements, while details can be found in [34–38] and in appendices C.1, C.2, C.3, C.4 and C.5.

To make the further discussion more clear, we briefly summarize the basics and formalism of relativistic kinetic theory and fluid dynamics in appendix A. We follow the notations used in Csernai's text book [42].

2.1 General aspects of Freeze Out

2.1.1 Time-like and space-like discontinuities in relativistic flow

A frequently used assumption is that the freeze out happens across a hypersurface, so it can be described as a discontinuity where the equation of state and kinetic properties of the matter change suddenly. This surface is an idealization of a transition layer of finite thickness, where the frozen out particles are formed, and the interactions in the matter become negligible. The thickness of this layer is of the order of the mean free path of particles. The dynamics of this layer is described in different kinetic models, such as Monte Carlo models [43, 44] or four-volume emission models [15, 45–48]. The zero thickness limit of such a layer is the idealized FO surface. Kinetic models for hadronic degrees of freedom indicate that such an idealization is meaningful only for collisions of massive heavy ions like Au+Au or Pb+Pb [43, 44]. The best justification for using an idealized hypersurface to describe freeze out can be given for the case, when we include quark-gluon plasma in our reaction model with rapid final hadronization which coincides with freeze out [49, 50].

Mathematically, surfaces can be represented in every point by a unit normal vector, $d\sigma^\mu$, which is orthogonal to the surface at that point. Hypersurfaces in the four dimensional space-time can be time-like or space-like depending on the nature of the normal vector of the surface. Unfortunately,

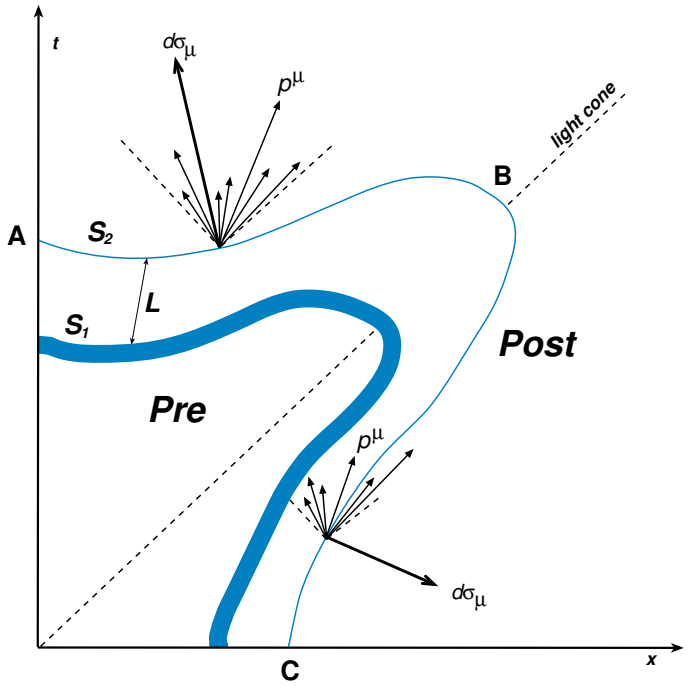

Figure 2.1: Flow across a freeze out layer. Between A and B the S_2 surface is time-like, while between B and C it is space-like. The momentum of particles is p^μ, the normal to the surface is $d\sigma_\mu$. Only those particles cross the surface which have their momentum pointing to the post FO side of the FO surface.

there is no unique convention for this classification in the literature. In this thesis and in each of our papers we will call a surface space-like when its normal is a space-like four-vector, i.e. $d\sigma_\mu d\sigma^\mu = -1$, while a time-like hypersurface has time-like normal, $d\sigma_\mu d\sigma^\mu = +1$.

In figure 2.1 the outermost surface, which is labeled with S_2, has both time-like (between points A and B) and space-like (between points B and C) regions.

The general theory of discontinuities in relativistic flow was first discussed by A. Taub [39] in 1948. In that work only discontinuities across propagating hypersurfaces were considered, i.e. surfaces with space-like normal vectors. Another type of change in a continuum is an overall sudden transition (e.g. phase transition) in a finite volume at a given time. This is represented by a hypersurface with a time-like normal. If one applies Taub's formalism to such time-like FO surfaces, one gets a usual Taub adiabat, but the equation of the Rayleigh line will yield imaginary values for the particle current across the front. Therefore, hypersurfaces with $d\sigma^\mu d\sigma_\mu = +1$ were thought to be unphysical, because the points of such a surface are not in causal connection with each other. In 1987 Taub's approach was finally generalized to both

types of surfaces [40], making it possible to take into account conservation laws exactly across any surface of discontinuity in relativistic flow. This approach also eliminates the imaginary particle currents arising from the equation of the Rayleigh line. When the equation of state is different on the two sides of the FO front, these conservation laws yield changing temperature, density and flow velocity across the front. Based on conservation laws and simple kinetic considerations the freeze out idealization was worked out in references [13–17, 29, 30, 41].

Partly based on these works we have generalized the kinetic freeze out treatment for *finite* time-like [35] and space-like [34] FO layers. Our new approach can handle both time-like and space-like freeze out processes on the same fully covariant footing. For more details see appendices C.4 and C.5.

Having a closer look on figure 2.1 one can observe that only those particles will reach the post FO side, which have their four-momentum outside the interacting pre FO volume. This condition is fulfilled for all particles emerging from a point situated on the time-like region, while some of the particles originating from a point on the space-like part of the FO surface will not leave the pre FO side. This introduces an extra difficulty when one studies the flow across space-like surfaces. In case of equilibrium on both sides of a hypersurface, there might be pre side particles, which have already visited the post side. This is a consequence of the fact that in the momentum distribution of a fluid in equilibrium all momenta are represented. Graphically this means that in every point the momenta of the particles occupy the full light cone. In principle, the same particle can cross a hypersurface several times. Therefore, special care is needed when we have non-interacting frozen out matter on the post side. In this case the back scattering is excluded, and thus, the post FO distribution function can contain only that part of the phase space, which falls into the post FO side.

2.1.2 Conservation laws across FO discontinuities

The energy-momentum tensor and baryon four-current change discontinuously across the FO surface. If the flow is not orthogonal to this surface, the four-vector of the flow velocity will also change [40, 49, 51]. In most of the cases the FO hypersurface is assumed to be time-like. If so, the method for the description of time-like detonations and deflagrations [40, 49, 51, 52] should be used.

The invariant number of conserved particles (world lines) crossing a surface element, $d\sigma^\mu$, is

$$dN = N^\mu \, d\sigma_\mu \ , \tag{2.1}$$

and the total number of all the particles crossing the FO hypersurface, S, is

$$N = \int_S N^\mu \, d\sigma_\mu \ . \tag{2.2}$$

This total number, N, and the total energy and momentum are the same on both sides of the FO hypersurface. If we insert the kinetic definition of the particle four-flow, N^μ,

$$N^\mu = \int \frac{d^3p}{p^0} \, p^\mu \, f_{FO}(x, p; T, n, u^\nu) \ ,$$

into equation (2.1), we obtain the Cooper-Frye formula [29]:

$$E\frac{dN}{d^3p} = \int f_{FO}(x, p; T, n, u^\nu) \, p^\mu d\sigma_\mu \ . \tag{2.3}$$

Here $f_{FO}(x, p; T, n, u^\nu)$ is the post FO phase space distribution of the frozen out particles, which is not known from the fluid dynamical model. Problems usually arise from the bad choice of this distribution. Evaluation of measurables requires that we use the correct parameters for the post FO phase.

Locally the system can be described by the currents of conserved densities, such as the baryon four-current, N^μ, and the energy-momentum tensor, $T^{\mu\nu}$. As we have already mentioned, these quantities are discontinuous across the FO surface, which is characterized at each point by its normal vector, $d\sigma^\mu$. In this case, the conservation laws take the following form:

$$[N^\mu d\sigma_\mu] = 0 \ , \tag{2.4}$$

$$[T^{\mu\nu} d\sigma_\mu] = 0 \ , \tag{2.5}$$

where $[A] \equiv A_2 - A_1$, A_2 and A_1 representing the same physical quantity on the post and pre sides of the surface, respectively. The continuity equations in the above form are valid for any well defined surface, not only for one connected to a discontinuity. Equations (2.4) and (2.5) are also known as the relativistic Rankine-Hugoniot equations, and they fix the parameters of the post FO phase space distribution, $f_{FO}(x, p; T, n, u^\nu)$. We also want to notice that particles can freeze out only if the entropy increases in such a process:

$$[S^\mu \, d\sigma_\mu] \geq 0 \ . \tag{2.6}$$

One usually assumes that both the pre FO distribution and the post FO distribution are local thermal distributions. However, this is not necessarily true on the post FO side.

A thermal post FO distribution for time-like freeze out surfaces does not lead to any significant problem, because all the possible future trajectories of a particle on such a FO hypersurface lead outside the interacting matter, therefore the particle necessarily freezes out, as we have seen in figure 2.1. Mathematically it can be demonstrated in the following way: in this case both p^μ and $d\sigma^\mu$ are time-like unit vectors, thus $p^\mu d\sigma_\mu > 0$, and the integrand in the above integrals is always positive on both sides of such a FO front. Thus, the Cooper-Frye freeze out formula (2.3) works nicely for any post FO distribution. For example, we may assume that f_{FO} is a Jüttner distribution [53], equation (A.6), as it was frequently done in the literature. However, the parameters T, n, u^μ, of the above distribution, f_{FO}, must be determined from the conservation laws, or Rankine-Hugoniot equations (2.4, 2.5) [40]. These important conditions were not fulfilled in the original work [29] and in many applications since, leading to violation of conservation laws.

The situation is more complicated in the case of freeze out across a space-like hypersurface. In this case, the four-momentum of particles, p^μ, may point both in the post and pre FO directions - see the point between B and C in figure 2.1. Now, the normal, $d\sigma^\mu$, is space-like while p^μ is time-like, and the product of the two, $p^\mu d\sigma_\mu$, can be either positive or negative. Thus, the integrand in the above integral (2.3) may change sign in the integration domain. This indicates that part of the distribution contributes to a current going back into the pre FO side, while another part is coming out of the front.

On the pre FO side p^μ is unrestricted and $p^\mu d\sigma_\mu$ may really have both signs, because we may assume that the FO front has a certain thickness and due to internal rescatterings inside this front a current is fed back to the pre FO side to maintain the thermal equilibrium there.

On the post FO side, however, we do not allow rescattering and back scattering any more. If a particle has passed the FO front, which in reality can be of finite width, it can not scatter back. Therefore, the post freeze out distribution must vanish for those momentum four-vectors, p^μ, which point backwards into the pre FO side, i.e. do not satisfy the condition: $p^\mu d\sigma_\mu > 0$ [13–17, 30, 41, 54] or

$$f_{FO}(x, p; T, n, u^\nu, d\sigma^\mu) = f_{FO}(x, p; T, n, u^\nu)\Theta(p^\mu \, d\sigma_\mu) \ , \qquad (2.7)$$

where Θ is the step function. Thus, this distribution cannot be a Jüttner- or other ideal gas distribution.

In reality the FO surface has to have a thickness and internal structure, which ensures that the local thermal equilibrium is maintained on its pre FO side – this involves back scattering of particles from the front to the pre FO side–, and at the same time it creates a momentum distribution on its post FO side, with no particles moving in the direction of the front. In [34, 35]

(appendices C.4 and C.5) we made the first step to develop a fully covariant kinetic description of the freeze out process through a freeze out layer of finite thickness.

Nevertheless, the above conservation laws have to be satisfied, even if the post FO distribution is not a local thermal distribution. This does not cause a large problem, because the post FO matter is dilute, its interactions are negligible, so the kinetic definitions of the energy-momentum tensor and conserved current are reliably applicable.

2.2 Kinetic Freeze Out models

2.2.1 Stationary space-like Freeze Out

As it was already mentioned, the dynamics of the FO in heavy ion collisions is a complicated process. However, one can study a simplified physical picture: the relativistic one dimensional expansion of a gas into vacuum, and then draw relevant conclusions for the FO in heavy ion collisions. Even this highly simplified model can be useful to understand qualitatively the main features of the process in question.

On the pre FO side the interacting gas is in local equilibrium, while on the post FO side the particles of the gas do not interact anymore, but freely stream towards infinity. Since the FO hypersurface is space-like ($d\sigma^\mu d\sigma_\mu = -1$) the post FO system is out of equilibrium. Inside the transition layer a gradual departure from local equilibrium takes place. We shall focus our attention on processes, which are taking place inside this layer.

2.2.2 The cut Jüttner distribution

As we have seen earlier in section 2.1.2, in the case of a space-like freeze out surface, the post FO distribution should vanish when $p^\mu d\sigma_\mu < 0$. The simplest way to take this into account is to consider a cut Jüttner distribution, suggested by K. Bugaev [41]:

$$f_{FO}(x,p;T,n,u^\nu) = \Theta(p^\mu\ d\sigma_\mu) f_{Jüttner}(x,p;T,n,u^\nu). \tag{2.8}$$

The step function, Θ, ensures that only particles with momenta pointing in the direction of the post FO side will contribute to the post FO distribution.

The baryon current and energy-momentum tensor on the post FO side were evaluated by Anderlik et al. in [13] correcting Bugaev's results [41]. Starting from the Bag model equation of state on the pre FO side, the authors evaluated the post FO parameters: n, T, u^ν, taking into account the non-decreasing entropy condition.

However, it is highly questionable that a distribution with such a sharp cut-off as the cut Jüttner one (2.8) is physical. Nature normally does not produce so sharp edges. Another way to introduce the cut-off Θ-function is to say that it is not a part of the post FO distribution, which might still be thermal, but the dynamics of the freezing out system is such that $\Theta(p^\mu d\sigma_\mu)$ necessarily appears in the modified Cooper-Frye formula. Such an approach has been presented in reference [54]. Nevertheless, it again ended up with an infinitely sharp cut-off in post FO quantities. It seems that the more physical assumption is that the post FO distribution is really cut-off type, i.e. satisfies equation (2.7), but it falls down gradually when $p^\mu d\sigma_\mu \to +0$ and does not have a sharp edge. As we will see in section 2.2.4, the cut Jüttner distribution can be reproduced in an oversimplified freeze out model, while the improved, more realistic model gives us a cut post FO distribution without sharp edge. Therefore, the cut Jüttner distribution should only be used as a qualitative tool.

2.2.3 The canceling Jüttner distribution

We have concluded in the previous section that it is hard to justify that a realistic physical process could produce a distribution of cut Jüttner type with an infinitely sharp cut-off. To overcome this problem the so-called Canceling Jüttner (CJ) distribution was recently proposed [27, 55], which solves the problem of negative contributions in the Cooper-Frye formula and has a smooth, physically more realistic form than the cut Jüttner one.

The canceling Jüttner distribution, f_{CJ}, is defined by subtracting an ordinary Jüttner distribution (A.6) with negative velocity, $-v$, from the original Jüttner distribution, and then multiplying the obtained result with the step function:

$$\begin{aligned} f_{CJ} &= \left(f_R^{Juttner} - f_L^{Juttner}\right)\Theta(p^\mu d\sigma_\mu) = \\ &= \frac{\Theta(p^\mu d\sigma_\mu)}{(2\pi\hbar)^3}\left(\exp\frac{\mu - p^\mu u_\mu^R}{T} - \exp\frac{\mu - p^\mu u_\mu^L}{T}\right), \end{aligned} \tag{2.9}$$

where $u_\mu^R = (\gamma, \gamma v, 0, 0)$ and $u_\mu^L = (\gamma, -\gamma v, 0, 0)$ in the rest frame of the front. The velocity parameter, v, of the CJ distribution is restricted to be positive.

In [27, 55] the following advantages of the CJ distribution were pointed out: 1.) It automatically includes the cut-off, but – opposite to the cut Jüttner type – it is a smooth, though rapid one, thus the distribution profile is more realistic. 2.) It resembles the distribution which was obtained from a kinetic freeze out model (see section 2.2.4 and [13, 15]) quite well, certainly better than the cut-Jüttner distribution. 3.) The formulation is still ana-

lytic and not more complicated than the one arising from the cut-Jüttner distribution.

The properties and applicability of the canceling Jüttner distribution were also demonstrated in [27, 55] by calculating post FO macroscopic quantities with this distribution as post FO distribution. On the pre FO side a Bag Model equation of state for quark-gluon plasma was used. Unfortunately, it turned out that the CJ distributon has limited applicability , because it was not possible to calculate post FO matter parameters for *all* initial pre FO values. Specially, the non-decreasing entropy condition, equation (2.6), was difficult to fulfill.

2.2.4 Idealized Freeze Out model with drain term

In the kinetic approach we want to determine the macroscopic properties of the system based on its microscopic features using the one-particle distribution function, $f(x,p)$. The time evolution of $f(x,p)$ is governed by the relativistic Boltzmann equation:

$$p^{\mu}\partial_{\mu}f(\vec{r},p) = C(x,p) \ , \tag{2.10}$$

where $C(x,p)$ is the collision integral, which describes the influence of collisions between the particles. If there is no interaction in the system, this term is zero.

In this section we will briefly discuss two models for the idealized freeze out process. Let us mention the common assumptions of these models:
A) In order to use Boltzmann's equation we consider only short range interactions among the particles.
B) We model the stationary flow, therefore no explicit time dependence is included.
C) The model calculations are done in one dimension, nevertheless, relativistic effects are taken into account.
Thus, from now x means only the x coordinate, not the four-vector, x^{μ}, as before, and all quantities have x dependence only.

The model can be easily visualized if we imagine an infinitely long tube with its left half ($x < 0$) filled with matter, while in the right half vacuum is maintained. We can remove the dividing wall at $t = 0$, and then the matter will expand into the vacuum. By continuously removing particles at the right end of the tube and supplying particles on the left end, we can establish a stationary flow in the tube. In the frame which is moving together with the particle flow, the particles gradually freeze out.

In references [13, 15–17] the freeze out kinetics in the right hand side of the tube was described assuming that the distribution function can be divided

into two components, $f_{free}(x,\vec{p})$ and $f_{int}(x,\vec{p})$ [45–47], where these components are the momentum distributions of free (frozen out) and interacting particles, respectively. The two components of the momentum distribution develop according to the following differential equations:

$$\begin{aligned} \partial_x f_{int}(x,\vec{p})dx &= -\Theta(p^\mu d\sigma_\mu)\frac{\cos\theta_{\vec{p}}}{\lambda} f_{int}(x,\vec{p})dx \ , \\ \partial_x f_{free}(x,\vec{p})dx &= \Theta(p^\mu d\sigma_\mu)\frac{\cos\theta_{\vec{p}}}{\lambda} f_{int}(x,\vec{p})dx \ , \end{aligned} \tag{2.11}$$

where $\cos\theta_{\vec{p}} = \frac{p_x}{p}$ in the rest frame of the front, and λ is the mean free path. Those particles, which move more forward, i.e. have a bigger $\cos\theta_{\vec{p}}$, have also a higher probability to freeze out. This reflects the fact that such particles have to cross a shorter distance before they get to a region with less interaction. While those, which move perpendicularly to the FO direction (here the x direction) will never freeze out. Neither do particles moving backward into the more interacting region. Therefore, the interaction part of the distribution will never vanish. Thus, complete physical freeze out is not realized. This feature of the model is due to neglecting the thermalization and rescattering in the interacting part. Nevertheless, the free component, f_{free}, at large distances reproduces the cut Jüttner distribution, as it was shown in [13, 15]. This model can be considered as a starting point, which reproduces oversimplified description of the freeze out process proposed in [41], and one can develop it to a more realistic model.

2.2.5 Freeze Out distribution with rescattering

As we pointed out in the previous section, in order to get a more realistic description of the freeze out process one has to include the effect of thermalization of the interacting component in the kinetic model [15–17]. For this aim we have to modify equations (2.11) including the collision term explicitly. However, we can take advantage of the relaxation time approximation. This means that the interacting component, $f_{int}(x,\vec{p})$, is relaxing towards an equilibrated Jüttner distribution, $f_{eq}(x,\vec{p})$, with the relaxation length λ'. Then, the two components of the momentum distribution develop according to the modified differential equations:

$$\begin{aligned} \partial_x f_{int}(x,\vec{p})dx &= -\Theta(p^\mu d\sigma_\mu)\frac{\cos\theta_{\vec{p}}}{\lambda} f_{int}(x,\vec{p})dx + \\ &\quad + \left[f_{eq}(x,\vec{p}) - f_{int}(x,\vec{p})\right]\frac{1}{\lambda'}dx \ , \\ \partial_x f_{free}(x,\vec{p})dx &= \Theta(p^\mu d\sigma_\mu)\frac{\cos\theta_{\vec{p}}}{\lambda} f_{int}(x,\vec{p})dx \ . \end{aligned} \tag{2.12}$$

The re-equilibration and the drain terms determine together the evolution of the interacting component, $f_{int}(x,\vec{p})$.

Here it is important to note that $f_{eq}(x,\vec{p})$ is not exactly the initial Jüttner distribution, but its parameters, $n_{eq}(x)$, $T_{eq}(x)$ and $u^{\mu}_{eq}(x)$, change as required by the conservation laws.

In [15–17] it was assumed that $\lambda' \to 0$, i.e. the immediate rethermalization limit was evaluated.[1] As an outcome of this model it was obtained that the arising post FO distribution, $f_{free}(x,\vec{p})$, will be a superposition of cut Jüttner type terms, from a series of gradually slowing down Jüttner distributions. This improved model enables complete freeze out. Although complete FO requires an infinite length, a large fraction ($\sim$ 90%) of the matter is frozen out within a distance of $x = 3\lambda$. Nevertheless, one should keep in mind that the models presented above do not have realistic behavior in the limit $x \to \infty$, due to their one dimensional character.

2.2.6 Volume emission model

In this section we will briefly present the volume emission model following the formalism introduced in [15]. The physical system looks the same as described in section 2.2.4, but the dynamics of the system is governed by a different set of equations. In the volume emission model a new quantity, the so-called escape probability is introduced:

$$\mathcal{P}(\vec{r},t,\vec{p}) \equiv e^{-\int_t^{\infty} \sigma v_{rel} \mathsf{n}(\vec{r}+\vec{v}t,t)dt} \ , \tag{2.13}$$

where $\mathsf{n} = N^0$ is the particle density in the calculation frame, $\vec{v} = \vec{p}/E$ is the velocity of the particle, σ is the total cross section and v_{rel} is the average relative velocity of particles.

We can justify the above equation in the following way: a particle is frozen out at time t if it does not collide anymore after this time. The probability for such a freeze out is described by a Poisson distribution:

$$P = W(0) = e^{-\rho N} \ , \tag{2.14}$$

where ρ is the probability of a collision and N is the total number of particles. Furthermore, ρN is the number of those particles, which our particle can meet on its way

$$\rho N = \int_t^{\infty} 4\sigma v_{rel} \mathsf{n}(\vec{r} + \vec{p}/Et, t)dt \ . \tag{2.15}$$

[1] In fact the immediate rethermalization limit is not immediate in a numerical solution but equals to the step-length. After each step (but not more frequently) the rethermalized distribution is re-evaluated, taking into account the particle, energy and momentum loss carried away by the frozen out particles. Thus, to achieve the most realistic description the step-length should not tend to zero. This is analogous to the treatment of viscosity in computational fluid dynamics.

Thus, P is given by expression (2.13). The interaction is included through the effective cross section, σ.

Now, the free particle distribution, $f_{free}(x,\vec{p})$, is given as a fraction of the total particle distribution

$$f_{free}(x,\vec{p}) = \mathcal{P} f(x,\vec{p}) \ , \tag{2.16}$$

while the interacting part of the particle distribution, $f_{int}(x,\vec{p})$, is defined as

$$f_{int}(x,\vec{p}) = (1-\mathcal{P}) f(x,\vec{p}) \ , \tag{2.17}$$

where $f(x,\vec{p}) = f_{free}(x,\vec{p}) + f_{int}(x,\vec{p})$.

Such a description leads to a set of integro-differential and integral equations. To solve these equations is a non-trivial numerical task. Nevertheless, some simple extrapolation approach to the solution was already performed. Detailed mathematical calculations were presented in [15].

An important advantage of the volume emission model is that it describes the FO process in a layer of finite thickness. Its main drawback resembles the one we have seen in the oversimplified model with drain term only - those parts of the initial spherical Jüttner distribution which move backward and orthogonal to the FO direction can not freeze out. The modification of the model is straightforward, we have to include thermalization and rescattering processes into the interacting component of the distribution function. Such an improvement in the volume emission model is rather complicated mathematically.

2.3 Modified Boltzmann transport equation

Recently considerable attention has been focused on the connection between the kinetic description of the freeze out process and the Boltzmann Transport Equation (BTE) [31, 56, 57]. The Boltzmann transport equation, which describes the evolution of a single particle distribution function, $f(x,p)$, may deal with both equilibrium and non-equilibrium processes in a 4-dimensional space-time volume element, like a freeze out layer. Thus, one would think that freeze out in energetic heavy ion collisions can be handled perfectly based on BTE.

We have investigated a dynamical freeze out description starting from the Boltzmann transport equation, and pointed out the basic limitations of the BTE approach. Our work on this topic was published in three papers [36–38], which can be found in appendices C.1, C.2 and C.3, respectively. We have also proposed a modification, the so-called *Modified Boltzmann Transport Equation* (MBTE), which can better handle freeze out in a finite layer. In paper C.2 [37] we have shown how the earlier ad hoc kinetic models of the

FO process [13, 15–17, 33], which were shortly described in the previous sections (2.2.4, 2.2.5 and 2.2.6), can be obtained from BTE and MBTE. The qualitative differences between the two approaches have also been discussed there, while some quantitative comparison is presented in paper C.3 [38].

In this section we will briefly introduce the modified Boltzmann transport equation. For a detailed derivation and for discussion of applicability, consult the above mentioned papers.

The BTE can be derived from the conservation of charges in a space-time domain, assuming the standard conditions [42]: (i) only binary collisions are considered, (ii) "molecular chaos" is assumed, i.e. the number of binary collisions at position x is proportional to $f(x,p_1) \times f(x,p_2)$ and (iii) $f(x,p)$ is a smoothly varying function on the scale of the mean free path.

It has to be taken into account that particles can scatter into the phase-space volume element around p, or can scatter out from this volume element. This is described by *gain*- and *loss*- collision terms in the BTE. We assume elementary collisions, where in the initial state two particles collide with momenta p_1 and p_2 into a final state of two particles with momenta p_3 and p_4. For the phase-space integrals we introduce the notation: ${}_{12}\mathcal{D}_3 \equiv \frac{d^3p_1}{p_1^0}\frac{d^3p_2}{p_2^0}\frac{d^3p_3}{p_3^0}$. Shortening the notation further, we will drop the momentum arguments of the phase-space distributions and will keep the indices only, i.e. $f(x,p_1)$ will be f_1 etc. Thus, the Boltzmann transport equation can be expressed as:

$$p^\mu \partial_\mu f = \frac{1}{2}\int {}_{12}\mathcal{D}_4 f_1 f_2 W_{12}^{p4} - \frac{1}{2}\int {}_{2}\mathcal{D}_{34} f\ f_2 W_{p2}^{34}\ , \tag{2.18}$$

where W_{ab}^{cd} is the invariant transition rate for the reaction $a+b \to c+d$.

In order to describe the freeze out, let us split up the distribution function, $f = f^i + f^f$, where f^f is the distribution function of the *free* or frozen out particles, while f^i is the *interacting* component [13, 31]. The particles belonging to the free component will not collide any more, thus, they do not appear in the initial state components of the collision integrals.

The gain term, $f_1\ f_2\ W_{12}^{p4} = f_1^i\ f_2^i\ W_{12}^{p4}$, populates both the interacting, f^i, and free, f^f, components. We introduce a FO probability, which feeds the free component, $\mathcal{P}_f \equiv \mathcal{P}_f(x,p)$, and thus the rest, $(1-\mathcal{P}_f)$, feeds the interacting one. The two components of f can be separated into two equations, and the sum of these two equations returns the complete BTE above:

$$\begin{aligned} p^\mu \partial_\mu f^f &= \frac{1}{2}\int {}_{12}\mathcal{D}_4 f_1^i f_2^i \mathcal{P}_f W_{12}^{p4}\ , \qquad (2.19)\\ p^\mu \partial_\mu f^i &= -\frac{1}{2}\int {}_{12}\mathcal{D}_4 f_1^i f_2^i \mathcal{P}_f W_{12}^{p4} \\ &\quad +\frac{1}{2}\int {}_{12}\mathcal{D}_4 f_1^i f_2^i W_{12}^{p4} - \frac{1}{2}\int {}_{2}\mathcal{D}_{34} f^i f_2^i W_{p2}^{34}\ . \end{aligned}$$

The free component does not have a loss term, because particles in the free component can not collide, i.e. the free component can not loose particles due to collisions. The first term of the second equation is a drain term, describing the escape or FO of particles from the interacting component. It is the inverse of the gain term for the free component. The last two terms influence the interacting component, and do not include the FO probability factors. These two terms drive the interacting component towards rethermalization.

However, the usual structure of the collision terms in the BTE is not adequate for describing a rapid freeze out process in a layer which is comparable to the mean free path. In this case the change of the particle distribution function, $f(x,p)$, in the direction normal to the layer is not negligible on this length scale, thus, assumption (iii) for BTE can not hold. The assumption of molecular chaos is also violated in a FO process because the number of collisions at point x is not proportional with $f(x,p_1)\times f(x,p_2)$, but it is delocalized in the normal direction with $f(x_1,p_1)\times f(x_2,p_2)$, where x_k $(k=1,2)$ are the origins of colliding particles, i.e. the space-time points where they had the previous collision.

As the FO proceeds, the number of interacting particles is constantly decreasing, correspondingly the mean free path is increasing. In fact, it reaches infinity when the FO is completed. Therefore, it is not possible to make the FO in finite layer of any thickness smooth enough to be modeled with the Boltzmann transport equation.

To describe that the phase space distributions change rapidly along the FO direction, the Modified Boltzmann Transport Equation (MBTE) is introduced:

$$
\begin{aligned}
p^\mu\partial_\mu f^f(x,p) &= \frac{1}{2}\int {}_{12}\mathcal{D}_4\mathcal{P}_f W_{12}^{p4}\ f_1^i(x_1,p_1)f_2^i(x_2,p_2)\ , \qquad (2.20)\\
p^\mu\partial_\mu f^i(x,p) &= -\frac{1}{2}\int {}_{12}\mathcal{D}_4\mathcal{P}_f W_{12}^{p4}\ f_1^i(x_1,p_1)f_2^i(x_2,p_2)\\
&\quad +\frac{1}{2}\int {}_{12}\mathcal{D}_4 W_{12}^{p4}\ f_1^i(x_1,p_1)f_2^i(x_2,p_2)\\
&\quad -\frac{1}{2}\int {}_{2}\mathcal{D}_{34} W_{p2}^{34}\ f_1^i(x,p)f_2^i(x_2,p_2)\ ,
\end{aligned}
$$

where $x_k=(t_k,\vec{x}_k)=(t-\gamma_k\tau_{coll},\ \vec{x}-\gamma_k\,\vec{v}_k\tau_{coll})=x-u_k\tau_{coll.}$, with $\vec{v}_k=\vec{p}_k/p_k^0$ and $u_k=(\gamma_k,\gamma_k\vec{v}_1)$. Here τ_{coll} is the mean collision time. This indicates that the particle k arrives at x starting earlier from another point x_k.

Although BTE and MBTE are very similar, the introduced modification is essential if the phase-space distribution has a large gradient. A simple general solution of the MBTE (2.20) has not been found, but it serves as a basis for simplified phenomenological kinetic models describing the FO process. Further details are given in papers C.1, C.2 and C.3.

2.4 Freeze out through a finite layer

As we have discussed in the previous section, the freeze out problem can be formulated in the framework of kinetic transport theory. It was shown in our recent papers [36–38] that the dynamical FO description can be based on the modified Boltzmann transport equation (MBTE), which is more suitable to describe the FO process than the BTE. However, this modification of the BTE makes it very difficult to solve the FO problem from the first principles. Therefore, it is important to build phenomenological models, which can explain the basic features of the FO process. Two of our papers [34, 35] were dedicated to this task.

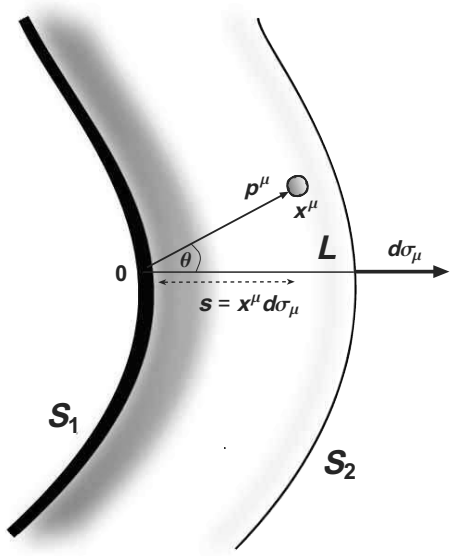

Figure 2.2: The picture of a gradual freeze out process within a finite freeze out layer of thickness L. $d\sigma_\mu$ is the normal vector of the FO layer. The particles may move in different directions outwards, which is indicated by the angle θ . The FO process starts on the inside boundary of the FO layer, S_1. This surface is the origin of the coordinate vectors of particles, x^μ. Within the finite thickness of the FO layer, L, the density of the interacting particles gradually decreases (illustrated by shading) and becomes zero at the outside boundary, S_2, of the FO layer.

The formulation of the kinetic freeze out models, which were briefly introduced in sections 2.2.4, 2.2.5 and 2.2.6 and described in details in [13, 15–17], were still based on the existence of a sharp FO hypersurface, and kinetic dynamics beyond. We have generalized the kinetic freeze out treatment for *finite* time-like [35] and space-like [34] FO layers. Our new approach is partly based on the earlier phenomenological models, but can handle both time-like and space-like freeze out processes on the same fully covariant footing. The

papers can also be found in appendices C.4 and C.5.

A schematic picture of a gradual freeze out process within a FO layer of finite thickness, L, is shown in figure 2.2. Particles start to freeze out when they reach the inside boundary of the layer, which is denoted by S_1 in the figure. The freeze out process is completed, when the particles finally cross the S_2 surface.

In the earlier models (see equations (2.11) and (2.12)), the following form of the escape probability was applied:

$$P_{esc} = \frac{\cos\theta_{\vec{p}}}{\lambda}\,\Theta(p^\mu d\sigma_\mu)\,, \tag{2.21}$$

where the cut-off factor, $\Theta(p^\mu d\sigma_\mu)$, eliminates the negative contributions, and λ stands for the mean free path. The angular factor, $\cos\theta_{\vec{p}}$, (or θ in figure 2.2) is the angle between the FO normal vector and $\vec{p}$. This escape probability is not Lorentz invariant, because of the angular factor. Furthermore, in the earlier models [13, 15–17] the complete FO required an *infinite* length ($L \to \infty$) after crossing a *sharp* FO surface.

We have generalized angular factor as

$$\cos\theta_{\vec{p}} \Longrightarrow \left(\frac{p^\mu d\sigma_\mu}{p^\mu u_\mu}\right), \tag{2.22}$$

where, p^μ is the four-momentum of a particle, $d\sigma_\mu$ is the normal of the FO layer and u_μ is the four velocity of the matter.

Then, taking into account that the FO happens in a *finite* layer of thickness L, we have introduced a Lorentz invariant escape probability or *escape rate*:

$$W_{esc} = \frac{1}{\lambda}\left(\frac{L}{L - x^\mu d\sigma_\mu}\right)\left(\frac{p^\mu d\sigma_\mu}{p^\mu u_\mu}\right)\Theta(p^\mu d\sigma_\mu)\,. \tag{2.23}$$

The derivation of equation (2.23) can be found in papers C.4 and C.5. We have also studied the behaviour of the momentum dependent part of the escape rate at different characteristic points of the FO hypersurface.

Applying the new invariant escape rate, equation (2.23), we can generalize the earlier kinetic models, e.g. equation (2.11) takes the form

$$\begin{aligned} d\sigma^\mu \partial_\mu f_i &= -\frac{1}{\lambda}\left(\frac{L}{L - x^\mu d\sigma_\mu}\right)\left(\frac{p^\mu d\sigma_\mu}{p^\mu u_\mu}\right)\Theta(p^\mu d\sigma_\mu) f_i\,, \\ d\sigma^\mu \partial_\mu f_f &= \frac{1}{\lambda}\left(\frac{L}{L - x^\mu d\sigma_\mu}\right)\left(\frac{p^\mu d\sigma_\mu}{p^\mu u_\mu}\right)\Theta(p^\mu d\sigma_\mu) f_i\,. \end{aligned} \tag{2.24}$$

If we describe the system in the rest frame of the front (RFF), where $d\sigma_\mu = (1,0,0,0)$ for a time-like and $d\sigma_\mu = (0,1,0,0)$ for a space-like FO surface,

Table 2.1: Time-like and space-like components in RFF

	Time-like	Space-like
$s \equiv (x^\mu d\sigma_\mu)$	t	x
$p^s \equiv (p^\mu d\sigma_\mu)$	p^0	p^x
$\partial_s \equiv (d\sigma^\mu \partial_\mu)$	∂_t	∂_x

equation (2.24) can be written as:

$$\begin{aligned} \partial_s f_i \, ds &= -\left(\frac{L}{L-s}\right)\left(\frac{p^\mu d\sigma_\mu}{p^\mu u_\mu}\right)\Theta(p^\mu d\sigma_\mu) f_i \, \frac{ds}{\lambda} \, , \\ \partial_s f_f \, ds &= \left(\frac{L}{L-s}\right)\left(\frac{p^\mu d\sigma_\mu}{p^\mu u_\mu}\right)\Theta(p^\mu d\sigma_\mu) f_i \, \frac{ds}{\lambda} \, . \end{aligned} \tag{2.25}$$

In equation (2.25) we have used the notations defined in table 2.1.

One can see that our approach handles both time-like and space-like freeze out processes. Let us make it clear that the thickness of the layer, L and the "distance", $s = x^\mu d\sigma_\mu$, which the particle travels from the crossing point at S_1 to the x^μ space-time point refer to distance or *length* in space only in the space-like case, while describing time-like FO process they actually represent *durations* in time. Thus, in equation (2.25) λ is the *mean free path* only in the space-like case, while it is the initial *mean collision time* in the time-like description.

The rethermalization in the interacting component can be taken into account via the relaxation time approximation, where the interacting component approaches an equilibrated Jüttner distribution, $f_{eq}(s)$, with a relaxation length (or relaxation time in the time-like case), λ_0. With these assumptions the evolution of the momentum distribution components can be expressed as:

$$\begin{aligned} \partial_s f_i ds &= -\left(\frac{L}{L-s}\right)\left(\frac{p^\mu d\sigma_\mu}{p^\mu u_\mu}\right)\Theta(p^\mu d\sigma_\mu) f_i \, \frac{ds}{\lambda} \\ &\quad + \quad [f_{eq}(s) - f_i] \, \frac{ds}{\lambda_0} \, , \\ \partial_s f_f ds &= \left(\frac{L}{L-s}\right)\left(\frac{p^\mu d\sigma_\mu}{p^\mu u_\mu}\right)\Theta(p^\mu d\sigma_\mu) f_i \, \frac{ds}{\lambda} \, . \end{aligned} \tag{2.26}$$

We may notice that the above equation is the generalization of equation (2.12).

To solve the above set of equations we assume *"immediate rethermalization"* [15–17, 33], because it leads to analytical results for the conserved

quantities, $N^\mu, T^{\mu\nu}$. The change of conserved quantities caused by the particle transfer from the interacting matter into the free matter has been obtained in terms of distribution of the interacting matter using equation (2.26).

We have performed calculations of the post FO distribution and the relevant quantities from this new model in the case of a baryonfree massless gas, where we have used a simple equation of state, $e = \sigma_{SB} T^4$. In this special case we could calculate the change of flow velocity and that of temperature. The resulting post FO phase-space distributions have been discussed for different escape probabilities and layer widths. Finally, we have compared the results to former calculations presented in [15–17, 33].

2.5 Determination of the FO hypersurface

Up to now we have discussed the freeze out through a known freeze out hypersurface (FOHS). Unfortunately, this is not always the case in real calculations.

The volume emission model, in principle, presents a method how to define freeze out: a particle is frozen out at time t and in the position $\vec{r}(t)$ if it does not collide anymore after this time. Similar ideas are also presented in [58]. Obviously, such a definition can not give a sharp FO hypersurface, particles will freeze out in some finite layer, as it was shown in the volume emission model. In order to define a sharp FO hypersurface we have to deal with elementary numerical cells instead of single particles.

In numerical calculations the local FO surface can be determined most accurately via self-consistent iteration [41, 59]. Nevertheless, any iteration scheme requires a FO condition, which determines when the matter in a local cell freezes out. Therefore, the first task is to find a reliable freeze out condition.

Experimental results show that the chemical FO points (defined from the best fit to all particle ratios) appear to be very close to the curve, defining the uniform energy distribution of outgoing particles, 1 GeV per particle (hadron) [60, 61].

In theoretical calculations it is usually assumed that the chemical and thermal freeze out happen simultaneously. The assumption of the simultaneous chemical and thermal freeze out has been justified for example in [62]. In this case it would be convenient to use the experimentally supported FO condition, $< E > / < N >= 1\,\mathrm{GeV}$, in self-consistent iteration scheme. Unfortunately, such an algorithm would be very complicated. Instead, the critical temperature condition, $T = T_{FO}$, is frequently used in order to determine the FO hypersurface [41, 59]. Experimentally this temperature can be found from the particle ratio analysis. Results of such an analysis are shown in figure 1.1.

The hydrodynamical description can much easier handle the thermal FO than the chemical FO. The chemical description in hydrodynamics would require the equation of state effectively taking into account all the hadronic species, i.e. $P = P(e, n_B, n_\pi, n_K, ...)$.

Thus, the determination of the FO surface is an involved task, both when it comes to the description of the correct physics and the technical implementation. In order to simplify the description it is an acceptable assumption that hadronization happens simultaneously with chemical and thermal freeze out [49, 50, 64]. It was pointed out in [49] that slow hadronization through a mixed quark-hadron phase contradicts to the experimentally observed short timespan and final size of the reaction zone. The only way to avoid this problem and hadronize the system is to assume that hadronization happens from supercooled QGP in a rapid process (within $1 - 2\,\mathrm{fm/c}$). Then, hadrons freeze out immediately. This is also confirmed by the large abundance of strange hadrons. If there would be time $(5 - 15\,\mathrm{fm/c})$ for hadronic reactions after hadronization, the strangeness overabundance would have disappeared in these hadronic reactions, which would re-establish flavour equilibrium in the hadronic phase.

The assumption of simultaneous chemical and thermal freeze out is also used by our group, when we identify the freeze out hypersurface in the large scale 3+1-dimensional system, which was produced by our CFD code in the second module of the Multi Module Model. The determination of the FOHS is done by analyzing the *complete* space-time history of the fluid dynamical stage. We use the critical temperature condition, $T = T_{FO}$, as freeze out criterion. The demanding task of FOHS identification has recently been completed by our collaborator, Bernd R. Schlei. Using the output data file from our fluid dynamical calculations, his code identifies the FOHS made of millions of fluid elements, and produces a data file which contains the space-time coordinates, the three components of velocity, temperature, pressure, energy- and baryon density and the four components of the normal of the surface for *each* fluid elements. This data file can be used in further calculations of the measurables. At the same time, the space-time evolution of the surface is visualized in a short movie. An example of such movie can be found in [65].[2] This movie corresponds to a gold-on-gold collision at 165 GeV energy with impact parameter $b = 0.5 \cdot 2\,R_{Au}$. The freeze out condition was $T_{FO} = 139\,\mathrm{MeV}$. One can see that at the late stages fluctuations start to dominate the evolution, space-time clusters are getting formed and then decay. This is a consequence of temperature fluctuations, caused by late negative pressure of the supercooled QGP in our fluid dynamical calculations priori to the FOHS determination. We have to find a reliable method how to exclude these clusters. Thus, work must still be done on the FOHS model

[2] To play the movie requires a QuickTime Player.

to avoid inaccuracies in the further calculation. We have already performed several tests of the freeze out hypersurface produced by the code, for example checked the normalization, i.e. the values of total net baryon charge and total energy from the fluid elements on the surface, and investigated how these quantities change as a function of time. As one expects, they increase first, as more and more matter freezes out, then saturate close to the theoretical total values. At later times fluctuations appear, just like in the visualization. The investigation of time dependence thus helps us to locate the earliest saturation time, and we can stop the further time evolution of the surface at that point. Then, the initial period can be used to calculate the post FO quantities and the resulting measurables. Such calculations have not been performed yet, since we have received the first freeze out hypersurface data only very recently.

Chapter 3

Collective flow in heavy ion collisions

In order to establish experimentally the properties of the hot and dense partonic matter created in heavy ion collisions, a wide range of variables of the system has to be measured. Due to the very brief existence and limited spatial extent of the generated plasma, however, its basic properties cannot be measured directly. Instead, it must be derived from the remnants of the collision, i.e. from the final state particles, which after the freeze out stage have reached the detectors. Several observables have been suggested as possible signatures of the formation of quark-gluon plasma based on theoretical predictions, and the experiments are searching for these signatures.

We start this chapter with a brief summary of the observables, which can carry information on the quark-gluon plasma. Then, from section 3.2 we will focus on a very important observable, the *collective flow*. After discussing the importance of anisotropic flow studies, in section 3.3.1 we will give an overview of the techniques, which are applied for flow analysis in experiments. We would like to mention in advance that the experimental methods have several weak points. Some of these will be pointed out when we describe the methods. A more detailed discussion of the possible problems connected to the experimental techniques will be given in section 3.3.2. After describing the experimental aspects of flow analysis, we will finally present our original results achieved in this topic in section 3.4. Our papers focusing on the collective flow [24, 149, 150] can be found in appendices C.6, C.7 and C.8.

3.1 Experimental observables

In general, the observables in a heavy ion collision can be divided into three main categories:

- Hadronic observables.
- Electromagnetic observables.
- Hard probes.

Each of the observables are characteristic of a certain stage in the collision, but they are not completely independent of each other. The hadrons emerge only in the final stage of the collision after they freeze out from the hadron gas, and thus carry direct information about the system at the time of freeze out. However, their properties are affected by the evolution of the system prior to the freeze out. The electromagnetic observables, on the other hand, may manage to escape without any further interaction due to their long mean free path relative to the size of the system, and thus emerge predominantly from the earlier hot stage of the collision. Finally, the initial stage of the collision is dominated by the collision dynamics of the produced partonic system, and the study of hard processes enable us to probe the very early parton dynamics and evolution of the initial stage of the system.

In the following the main observables, which might be relevant at ultra-relativistic energies, will be briefly introduced.

3.1.1 Hadronic observables

The hadronic observables are often referred to as *soft* probes of the heavy ion collision, as they are mostly connected to the non-perturbative aspects of QCD. They deal with the global characteristics of the system such as particle production, particle abundances and spectra, collective phenomena and correlations. These observables are the most sensitive to the properties of the quark-hadron phase transition.

Particle multiplicity

One of the most important and fundamental observables in a heavy ion collision is particle multiplicity. By measuring the number of particles produced in the collision, one can determine the energy density of the system. From a theoretical point of view this is important, since it enters the calculation of many other observables. On the experimental side, the particle multiplicity fixes the detector performance, and thus the accuracy, with which many of the observables can be measured.

Particle spectra and correlations

Most of the particles emitted in a heavy ion collision are hadrons which decouple from the collision region during the freeze out stage. Hence, by

measuring the different particle spectra, one obtains information about the chemical and kinetic freeze out distributions. From these observables, one can derive quantities like the freeze out temperature and chemical potential, flow components and the size of the system.

Since these distributions are also highly constrained by the dynamical evolution of the system, they will also yield information about the early stages of the collision [66–68]. Moreover, the final momentum distributions may provide detailed information about the time evolution of the collision system [69].

Essential information about the colliding system is obtained from studying its evolution in time and space. The size and expansion results from the work of pressure gradients within the system, and hence reflects directly the underlying equation of state. This can be obtained directly by particle interferometry or correlations. By these methods one can measure the final size of the fireball, gain insight about its expansion and phase-space density and provide information about the timing of the hadronization.

Furthermore, the *anisotropic flow* is sensitive to the degree of thermalization achieved in the system. In general it describes the azimuthal asymmetry of the particle production, and builds up through re-scattering in the evolving system, which converts the spatial anisotropy into momentum anisotropy. A rapid expansion of the hot system will destroy the original anisotropy and reduce the following momentum anisotropy. Thus, by measuring the anisotropic flow, information about the early stages of the collision is obtained, and one can find out whether local thermalization is reached followed by a collective hydrodynamic expansion.

Fluctuations

Like any other measured physical quantity, the observables in a heavy ion collision are also subject to fluctuations. These fluctuations themselves can provide useful information about the collision, because they are generally system dependent. One of these observables is the fluctuation of certain particle ratios, as they give access to information about the abundance of resonances at the chemical freeze out [70]. Furthermore, by measuring the charge fluctuations per unit degree of freedom of the system in a heavy ion collision, one can gain knowledge whether a QGP phase was created [71]. The main idea is that in a QGP phase the system would consist of quarks and gluons, which means that the unit of charge is 1/3, while in a pure hadronic phase it will be 1. The fluctuation in the net charge depends on the squares of the charges, therefore, it is strongly dependent on the phase it originates from.

3.1.2 Electromagnetic observables

Electromagnetic observables, like photons, may carry unperturbed information about the source in which they have been produced. The mean free path of photons in the medium is large enough to escape the system without any further interaction. These so-called direct photons provide a powerful probe of the evolution of the collision. However, the experimental feasibility is dominated by a severe background from the radiative decay of neutral pions ($\pi^0 \rightarrow \gamma\gamma$). Results from WA98 experiment indicates that the task of extracting the direct photons at SPS energies is feasible [72]. Recent results from the PHENIX experiment at RHIC show a direct photon signal above the expected background in central Au+Au events [73].

3.1.3 Hard probes

During the initial non-equilibrated stage of an energetic heavy ion collision the reaction dynamics is dominated by hard processes within the interacting partonic system. The study of such processes might give information on the very early parton dynamics and the evolution of the QGP phase. In contrast to the hadronic observables, hard probes involve only a limited number of highly energetic colliding partons, and are theoretically treated by perturbative QCD.

Jet production

During the interpenetration of two high-energy colliding nuclei, the partons within the projectiles interact with each other in hard two-to-two processes, and the initial parton momentum is transferred into final state partons or photons. Each of these final state partons will then emerge back-to-back from the collision region and radiate energy, because of their colour charges, before they finally hadronize into a number of colourless hadrons. The resulting cluster of particles is commonly referred to as jets.

High transverse energy jets produced in a heavy ion collision are expected to loose major parts of their initial energy when traversing the collision region prior to the freeze out phase. Therefore, studying jet production can help us to determine the QCD medium effects acting on a colour charge traversing a medium of colour charges, in analogy to the Bethe-Bloch method of QED. By comparing the cross section for jet production in heavy ion collisions with that in p+p collisions at the same center of mass energy, one can identify these medium modifications of the jet properties, which characterize the hot and dense nuclear matter in the initial stage of the collision region.

Several observables have been proposed as probes for the energy loss of the fast moving partons in the medium of deconfined color charges [74–

76]. In particular, this energy loss should be visible as a reduced yield, or *quenching*, of high momentum hadron jets in central A+A collisions. This effect has indeed been observed at RHIC [77]. The measurements show that central collisions between gold nuclei exhibit a very significant suppression of the high transverse momentum component as compared to nucleon-nucleon collisions. This observation indicates a substantial energy loss of the final state partons or their hadronic fragments in the medium generated by high energy nuclear collisions.

Heavy quark production

Heavy quarks, like charm and bottom, provide a probe which is highly sensitive to the collision dynamics. Heavy quark production is a perturbative phenomenon which takes place on a time scale of the order of the inverse quark mass. The relative long lifetime of the charm and bottom quarks allows them to live through the thermalization phase of the QGP, and thereby also be affected by its presence. Heavy quark-antiquark pairs may form *quarkonium* states with binding energies comparable to the temperature of the QGP, implying large quarkonium break-up and suppression.

Typical observables including heavy quark production are the total production rates, transverse momentum distributions and kinematic correlations between the heavy quark and antiquark. These observables have to be compared to those of p+p and p+A collisions in order to extract information on the properties of the hot and dense matter.

The observables connected to the heavy quark production will become increasingly important at LHC energies, as the center of mass energy will be sufficient to abundantly produce the heavy charm and bottom quarks and their bound states.

3.2 Collective flow in heavy ion collisions

Among the above mentioned experimental measurables we are particularly interested in the collective flow. Recently, the study of collective flow in nuclear collisions at high energies has attracted increased attention of both theoreticians and experimentalists. In this section we will discuss this phenomenon in more details both from theoretical and experimental point of view.

The occurrence of collective flow in relativistic heavy ion collisions was theoretically predicted more than 30 years ago [79, 80] and was first observed beyond doubt in 1984 by the Plastic Ball collaboration at LBL [81]. Subsequently, using the brilliant method worked out by Danielewicz and Odyniecz based on the physical properties of heavy ion collisions [82], the collective flow

was possible to detect in smaller samples and in a wide range of detectors. Directed flow was then extensively studied and reviewed at lower beam energies [83]. With time a variety of collective flow patterns were detected, the "squeeze out", the "elliptic flow", the "antiflow" or "3rd flow component", etc. The increasing complexity of flow patterns naturally led to attempts to classify the flow patterns in a more systematic way, and not just following the new experimental observations.

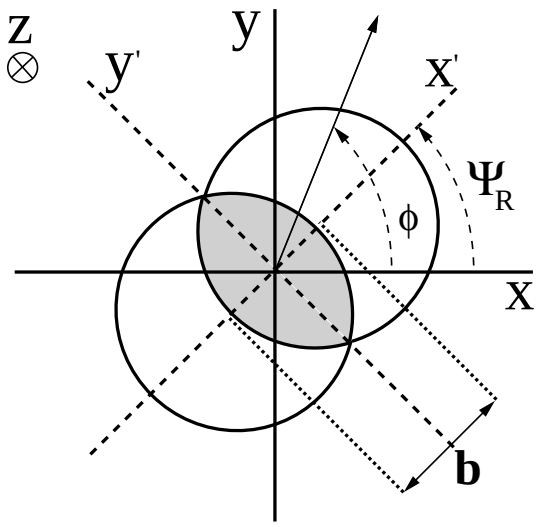

Figure 3.1: Schematic view of a collision in the transverse plane. Ψ_R is the azimuthal angle of the reaction plane, while ϕ is that of an outgoing particle. The reaction plane is the $[x', z]$ plane, $\mathbf{b}$ is the impact parameter.

Anisotropic flow is defined as azimuthal asymmetry in particle distributions with respect to the reaction plane. It appears very convenient to describe the azimuthal distribution of particles at fixed rapidity, y, by means of a Fourier expansion [84–86], and then azimuthal anisotropies can be classified via the coefficients, $v_n(y)$, of this Fourier expansion [86, 87]:

$$E\frac{d^3N}{d^3P} = \frac{1}{2\pi}\frac{d^2N}{p_t dp_t dy}\left(1 + 2\sum_n v_n \cos\left(n\,\Phi\right)\right) \ , \tag{3.1}$$

where Φ is the azimuth angle of an emitted particle with respect to the true reaction plane of the event. Anisotropic flow components corresponding to the first two harmonics, v_1, v_2, play a very important role and we use special terms for them: *directed* and *elliptic flow*, respectively. In experiments anisotropic transverse flow manifests itself in the distribution of $\phi = \Phi + \Psi_R$, where ϕ is the measured azimuth for a track in detector coordinates, and Ψ_R

is the azimuth of the reaction plane in the event, which varies event by event in the coordinate frame of the detector. A schematic view of a non-central collision in the transverse plane is shown in figure 3.1.

Using the above definition, equation (3.1), the coefficients have a transparent meaning [86]:

$$v_n = \langle \cos(n(\phi - \Psi_R)) \rangle \ , \tag{3.2}$$

so that the first coefficient, v_1, is $v_1 = \langle p_x/p_t \rangle$ and the the second coefficient, v_2, is $v_2 = \langle (p_x/p_t)^2 - (p_y/p_t)^2 \rangle$, where the average is taken over all emitted particles in a given rapidity, y, and transverse momentum, p_t, bin in all events. Ψ_R can not be directly measured, and randomly takes any value in $[0, 2\pi]$ due to the random direction of the impact parameter vector of the event.

3.2.1 Anisotropic flow as a QGP signal

Anisotropic flow is a powerful tool in the quest for the quark-gluon plasma and the understanding of bulk properties of the system created in heavy ion collisions. There has been a huge progress in the theoretical understanding of the relation between the appearance and development of flow during the collision evolution, and processes such as thermalization, creation of the quark-gluon plasma, phase transitions, etc. [88–99].

Important insights into the evolution of the reaction zone may be obtained from the study of the anisotropic flow, most of which is believed to originate at the early stages of the collision process [84, 93, 100]. The overlapping area of two nuclei in a non-central collision has a characteristic almond shape [100] in the transverse plane, resulting in azimuthally anisotropic pressure gradients, and therefore a non-trivial flow pattern. The pressure-driven expansion tends to reduce the spatial anisotropy and tries to restore spherical shape, provided that the thermalization sets in rapidly and the hydrodynamic description is appropriate [84, 87, 94]. When it becomes spherical, apparently, the anisotropic flow stops to develop. This feature is often referred as *self-quenching* [100]. The self-quenching makes the flow particularly sensitive to earlier stages of ultra-relativistic heavy ion collisions, when the spatial anisotropy and pressure gradients are the greatest.

As it was shown, the development of flow is closely related to the pressure gradients, and thus, to the equation of state of the hot and dense matter formed in the collision [83, 94]. Therefore, collective flow is believed to be a promising signal to detect the creation of the quark-gluon plasma [95–99]. At larger transverse momenta, measurements of azimuthal anisotropy are also relevant to the observation of jet quenching [101, 102]. An increased attention to collective flow has resulted in significant improvements in the techniques and methods of analysis and presentation of the experimental

data. PHENIX, PHOBOS and STAR experiments at RHIC have produced a wealth of information on the flow components [101–115].

Beside our theoretical analysis, in this chapter we will briefly present the recent techniques used in these experiments to analyze flow components, and we will summarize the most important experimental results as well.

3.2.2 The third flow component

As it was discussed in section 3.2.1 the flow pattern carries information on the pressure development during the collision including the early stages.

The phase transition from hadronic matter to QGP is connected to a decrease of pressure according to most theoretical estimates, not only in strong first order phase transition models, but even if we have a smooth but rapid gradual transition. This reduced pressure around the phase transition threshold are known for a long time [116], and it was emphasized as a possible QGP signal. This "soft point" of the equation of state might be possible to observe in excitation functions of collective flow data [117, 118].

In this section we want to discuss another consequence of the same softening in the equation of state, which is a recently identified new flow pattern – the so-called *third flow component* [95]. This flow pattern appeared in theoretical fluid dynamical calculations with QGP formation, and was possible to observe in experimental data as well, but it was not discussed earlier [117, 119–121].

The directed transverse flow was clearly detected in heavy ion collisions from energies of 30 AMeV to 165 AGeV [122–129]. At BEVALAC/SIS energies ($E_{lab} = 0.1$ AGeV-1 AGeV) and at lower AGS energy ($E_{lab} = 10.7$ AGeV) the directed flow resulted in a smooth, nearly linear p_x or v_1 vs. y dependence, and appeared as an almost straight line connecting the minimum at y_{targ} the maximum at y_{proj} and. Conventionally, we will call this type of flow, for which the slope dv_1/dy is positive, *normal* flow, in contrast to the *antiflow* for which $dv_1/dy < 0$ in the midrapidity region.

At higher energies deviations from this straight line behavior have been observed [95]. The shape of directed flow changes dramatically in the case of protons and exhibits a characteristic, so-called "wiggle" [130] structure in the midrapidity region, where the slope is negative and the sign of directed flow changes three times. Surprisingly, the directed flow of pions does not follow the same behaviour as that of protons. To illustrate this, the dependence of directed flow, v_1, on rapidity, y, is shown in figure 3.2 for 40 and 158 AGeV data from lead-lead collisions at SPS for pions and protons, reported by the NA49 Collaboration [128].

In theoretical calculations the important feature of the third flow component is that it clearly shows up in fluid dynamical calculations with QGP

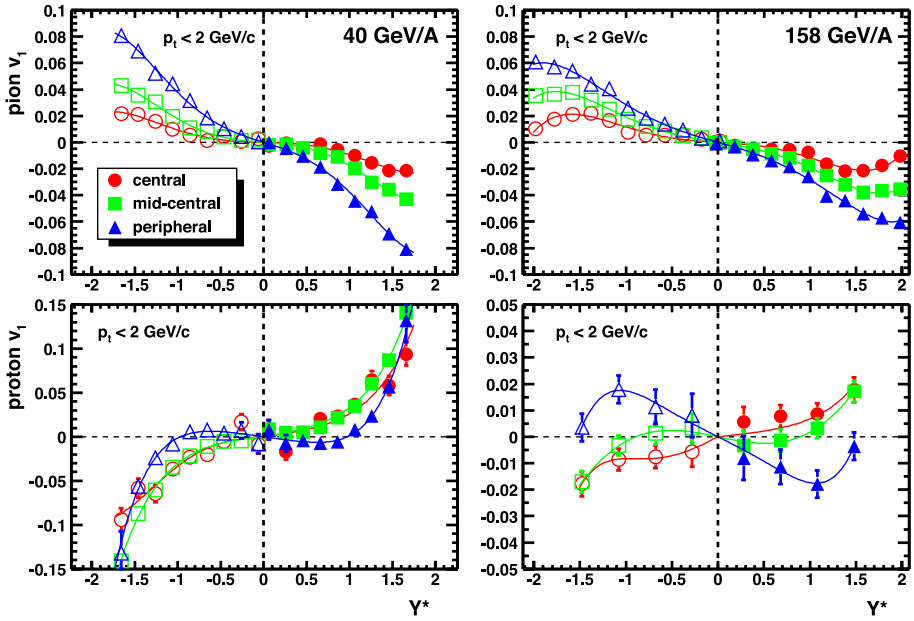

Figure 3.2: Pion (top) and proton (bottom) directed flow in Pb + Pb collisions at 40 AGeV (left) and 158 AGeV (right). Open points are reflected at mid-rapidity. Please note the different scale on the the two proton plots [128].

equation of state, while it does not appear using only hadronic equation of state [95].[1] Therefore, the appearance of the "wiggle" structure in the directed flow results is believed to be an important signature of the QGP creation. We will present recent directed flow results from RHIC in section 3.3.

Possible source of the third flow component

A possible source of the third flow component has been proposed in [95]. If QGP is created in our collision, the soft and compressible QGP forms a rather flat disk orthogonal to the beam axes, which then starts to expand in the direction of the largest pressure gradient. At small but finite impact parameters we may assume that this disk is tilted. The direction of fastest expansion will stay in the reaction plane, however, it will deviate from both the beam axis and the usual transverse flow direction. Thus, a third flow component might develop from the tilted and strongly Lorentz contracted initial state governed by the large pressure gradient.

[1] Such fluid dynamical calculations were done much before the experiments, and the first quantitative flow predictions [119] preceded the experiments by 6 years and gave rather good agreement with the data.

The concept of tilted fireball was proposed initially in the so-called *firestreak* models [131, 132]. The idea behind is rather simple and based on momentum conservation. Without going into mathematical details one can understand it in the following way: first, let us divide the projectile and target into streaks parallel to the beam direction. In the center of mass frame in one streak the fragments of matter from the target and the projectile will have the same absolute values of rapidities, but different momenta, since they in general contain different amount of matter. The situation is illustrated in figure 3.3.

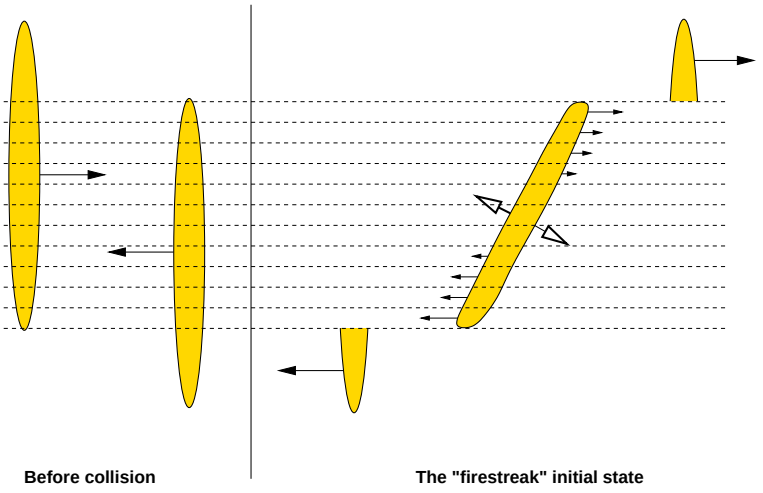

Figure 3.3: Tilted "firestreak" initial state. The direction of the largest pressure gradient stays in the reaction plane, but deviates from both the beam and the usual transverse flow directions. Such initial conditions may lead to the creation of the third flow component [95].

If the collision happens so fast, that there is no interaction between streaks, then the momentum conservation does allow the complete stopping, i.e. the piece of matter in the final streak will have a momentum defined by momentum conservation, and correspondingly its center of mass will move with some rapidity. Crossing the participant region along x axes in the reaction plane we will see that in the middle of the reaction zone the final streak rapidities are small, since here the target and projectile fragments were almost equal, while at the edges of the participant region the final streaks move rather fast.

This firestreak scenario might be a good qualitative description for the initial stages of the heavy ion collisions until the local thermalization is achieved. When the matter is locally thermalized and the pressure is build up, we can not neglect hydrodynamical expansion, which will smear out this initial distribution producing more or less spherical fireball before the freeze out

process starts. However, the hydrodynamical expansion will initially start in the direction of the largest pressure gradient, as indicated in figure 3.3, and together with the initial velocity field it might produce the third flow component identified in [95].

We have discussed the third flow component as a QGP signal in paper [133], which can be found in appendix C.6 too. In the paper we also show that this interesting flow pattern can be produced in our Multi Module Model calculations using the the Effective String Rope Model [12, 18] as initial state module.

3.3 Experimental methods and results

While an increasing attention was focused on the collective flow in energetic nuclear collisions, the techniques and methods of flow analysis and presentation of the experimental data have also gone through significant improvements. Several different techniques have been used to calculate flow components. In this section we will shortly introduce the basic ideas of the frequently used methods, and will present the most recent experimental results.

In flow analysis a very important, however, far not trivial task is the identification of the reaction plane. A physically well established and successful method for this purpose was introduced by Danielewicz and Odyniecz [82]. The Danielewicz-Odyniecz method constructed an estimated reaction plane, which is frequently called the event plane, $\Psi_{\{EP\}}$, using the the momentum vectors of all detected particles, introducing a rapidity dependent weighting, where the sign of the center of mass rapidity was crucial, and by eliminating self correlations. This weighting, in principle, should also be used in all other methods based on Fourier expansion, which operates with an event plane [87], especially for odd harmonics.

After identifying the event plane, the Fourier coefficients in the expansion of the azimuthal distribution of particles with respect to this plane can be evaluated. Because the finite number of detected particles produces limited resolution in the angle of the measured event plane, these coefficients must be corrected up to what they would be relative to the real reaction plane. This is done by dividing the observed coefficients by the event plane resolution, which is estimated from the correlation of the planes of independent subevents [82], i.e. sub-groups of the particles used for the event plane determination. Also, if the detector does not have full azimuthal acceptance, the acceptance bias has to be removed.

Many of the methods used recently do not exploit the information in the rapidity distribution of the emitted particles, which makes the evaluation of odd harmonics particularly problematic.

3.3.1 Techniques for analyzing v_n

Pairwise correlation method

Because of the difficulties one might run into while estimating the reaction plane, there were attempts to analyze flow components without using any event plane. Wang *et al.* suggested that the flow coefficients can be obtained by the *pairwise correlation* [134] of all particles detected in the experiment without referring to the reaction plane. This two-particle correlation method produces the squares of the coefficients, so that one has to take the square root of the correlation effect:

$$v_n^2 = \langle \cos\left[n(\phi_i - \phi_j)\right] \rangle_{i \neq j} \ , \tag{3.3}$$

where the average is taken over all possible particle pairs. The method has the advantage that the reaction plane does not need to be determined or estimated by an event plane. Self-correlations are removed by definition, however, so-called two particle non-flow effects are also included in v_n, which makes this method less accurate, and less attractive for experimentalists. Furthermore, this method is not able to determine the sign of v_n, thus it is not adequate for the determination of odd harmonics, where the azimuthal anticorrelation at opposite rapidities is an essential physical information.

Event plane method

The essence of the *event plane method* [87] is first to estimate the reaction plane with an event plane, and then to investigate the correlation of particles with respect to this plane. The flow components are evaluated as follows:

$$v_n^{obs} = \langle \cos\left[n(\phi_i - \Psi_n)\right] \rangle \ , \tag{3.4}$$

where Ψ_n is the azimuth of the observed event plane of order n and v_n^{obs} refers to the *observed* flow coefficients.

It was emphasized earlier in this section that the observed event plane may significantly differ from the true reaction plane, therefore, the observed coefficients, v_n^{obs}, have to be corrected by the resolution of the event plane caused by the finite multiplicity of the events. The resolution is estimated by measuring the correlations of the *event planes of subevents.*

In principle, the Danielevicz-Odyniecz method [82] could be utilized for the estimation of the event plane. Nevertheless, in [87] a slightly different technique was introduced.[2] The method uses the anisotropic flow itself to

[2]For the case of $n = 1$, equations ((3.5) and (3.6)) are equivalent to obtaining Ψ_1 for directed flow from [82]

$$\vec{Q} = \sum_i w_i \vec{p_t}/|\vec{p_t}|,$$

where the sum is taken over all particles.

determine the event plane. It also means that the event plane can be determined independently for each harmonic of the anisotropic flow. On the other hand, physically only one reaction plane exists in one event, so the determined event planes should be identical! The event flow vector Q_n and the event plane angle Ψ_n from the nth harmonic of the distribution are defined by the equations

$$\begin{aligned} Q_n \cos(n\Psi_n) &= X_n = \sum_i w_i \cos(n\phi_i) \ , \\ Q_n \sin(n\Psi_n) &= Y_n = \sum_i w_i \sin(n\phi_i) \ , \end{aligned} \tag{3.5}$$

thus the azimuth of the event plane of order n is

$$\Psi_n = \frac{1}{n} \tan^{-1} \left(\frac{\sum_i w_i \sin(n\phi_i)}{\sum_i w_i \cos(n\phi_i)} \right) \ . \tag{3.6}$$

The sums go over all particles, i, used in the event plane determination, and w_i are weights. In general the weights are also optimized to make the reaction plane resolution as good as possible. Usually the weights for the odd and even harmonics are different. Optimal weights were discussed in [135]. In the case of the odd harmonics the signs of the weights are reversed in the backward hemisphere, while for the even harmonics the signs of the weights are not reversed.[3]

In the flow analysis performed by the NA49 Collaboration [128, 129] the weights, w_i, have been taken to be p_t for the second harmonic and y in the center of mass for the first harmonic. Similar weighting was used in the recent calculations done by the STAR Collaboration [105, 111]. For even harmonics weights proportional to p_t were used up to 2 GeV/c and constant above that. For the odd harmonics the weights were proportional to the pseudorapidity, η for $|\eta| > 1$.

The next step is to study the particle distributions with respect to the event planes using equation 3.4. Note that for a given n the corresponding Fourier coefficient v_n^{obs} can be evaluated using the reaction planes determined from any harmonic m, with $n \geq m$, if n is a multiple of m. If $n > m$, the sign of v_n^{obs} is determined relative to v_m. That is, the first harmonic plane can be used, in principle, to evaluate all v_n^{obs}. The second harmonic plane can be used to evaluate v_2^{obs}, v_4^{obs}, etc.

To get the *real* flow components, v_n, with respect to the *real* reaction plane, one has to divide v_n^{obs} with the event plane resolution. The subevent

[3]The reason is that for symmetric collisions reflection symmetry says that particle distributions in the backward hemisphere of the center of mass should be the same as in the forward hemisphere if the azimuthal angles of all particles are shifted by π.

method, which is widely used for this purpose, was originally used in the Danielevicz-Odyniecz method [82] to determine the accuracy of the estimated reaction plane from the data. Applying it in the Fourier expansion method, there are several ways to choose subevents. Most trivially one can divide each event *randomly* into two subevents. Particles from the event can also be separated into subevents based on the *sign of charge*, which would lead to the strongest anisotropic flow due to non-flow effects of resonance decays. The choice of subevents might also be based on the experimental setup itself. Particles captured by the same detector might form a subevent and give a basis to determine the subevent plane, like in the STAR experiment [105, 111], where event planes were identified for the main Time Projection Chamber (TPC) and for the Forward Time Projection Chambers (FTPCs). This method of choosing subevents is widely applied recently, but it is qustionable if one can separate real physical effects from random fluctuations using such subevents.

When the two subevents, A and B, are formed, the azimuth of the subevent planes, ${\Phi_n}^A$ and ${\Phi_n}^B$, can be determined using equation (3.6), where the sums now are taken over the particles in the given subevent. The event plane resolution for the nth harmonic, R_n, can be expressed as

$$R_n = \sqrt{\langle \cos\left[n({\Phi_m}^A - {\Phi_m}^B)\right]\rangle} \ , \tag{3.7}$$

where $n = km$, and k is not necessarily equal to 1.

Now, the real flow components, v_n, is calculated as

$$v_n = v_n^{obs}/R_n \ . \tag{3.8}$$

The event plane resolution is always less than one, $R_n < 1$, and thus dividing by it raises the observed flow values. For more details consult [87, 129].

The event plane method is valid for all flow components and correct when correlations induced by flow are significantly larger than *non-flow* correlations, such as Bose-Einstein (Fermi-Dirac) statistics, final state Coulomb interactions, resonance decays, jets etc. The effects of these non-flow correlations may be large at SPS and RHIC energies, as it was shown in [136, 137]. The event plane method has been modified to take into account part of these effects. In particular, correlations from momentum conservation are subtracted following the procedure described in [138]. Nevertheless, the concept of removing correlations arising from momentum conservation is very dubious, as momentum conservation is the basis of fluid dynamics. If one by one we subtract 2, 3,... N-particle correlations ($N \to \infty$) caused by momentum conservation, then nothing would remain from the collective momentum conservation.

Multiparticle correlations–Cumulant method

Recently, a *multiparticle correlation* or *cumulant method* [139–141] is widely used. This method is supposed to minimize non-flow effects, which are not correlated with the reaction plane, however, it has larger statistical errors than the two-particle analysis. The basic idea of the method is to extract flow components from multiparticle azimuthal correlations. Naturally, the measured k-body correlations also consist of contributions due to flow and non-flow effects. It is claimed in [139–141] that by performing a cumulant expansion of the measured correlations, it is possible to disentangle the flow contributions from the other, unwanted sources of correlations. For example, at the level of four-particle correlations, one can remove *all* non-flow two- and three-particle correlations, keeping only correlations due to flow, plus a systematic uncertainty arising from non-flow *four*-particle correlations, which is expected to be small. However, the subtraction of the so-called non-flow effects is debatable, and can be justified only if the event, which causes it, happens outside (before or after) the fluid dynamical stage of the reaction. It is doubtful that the method eliminate *only* non-flow correlations. We will discuss this and other problems with the cumulant method in more details in section 3.3.2. The cumulant method provides several independent estimates of the flow components, which are labeled by the order k at which the cumulant expansion is performed: for instance, $v_2\{4\}$ denotes the estimate of v_2 using cumulants of 4-particle correlations, etc. Generally speaking, the systematic error due to non-flow correlations is supposed to decrease as the order k increases, at the expense of an increased statistical error.

To demonstrate the method, let us consider a simplified situation, where one measures the average value of the flow, v_n, with a detector, which has perfect azimuthal symmetry. The lowest order estimate of v_n from two-particle correlations, $v_n\{2\}$, is then defined by

$$v_n\{2\}^2 \equiv \left\langle e^{in(\phi_a-\phi_b)} \right\rangle \tag{3.9}$$

where the brackets denote the average over pairs of particles, (a, b), emitted in a collision, and over all events in an event sample[4].

Higher order estimates are obtained from two complementary multiparticle methods. The first one [140] measures the flow harmonics separately, either v_1 or v_2. For instance, the four-particle estimate $v_n\{4\}$ is defined by

$$\begin{aligned} -v_n\{4\}^4 \equiv & \left\langle e^{in(\phi_a+\phi_b-\phi_c-\phi_d)} \right\rangle \\ & - \left\langle e^{in(\phi_a-\phi_c)} \right\rangle \left\langle e^{in(\phi_b-\phi_d)} \right\rangle \\ & - \left\langle e^{in(\phi_a-\phi_d)} \right\rangle \left\langle e^{in(\phi_b-\phi_c)} \right\rangle , \end{aligned} \tag{3.10}$$

[4]Note that $v_n\{2\}$ is consistent with the value given by the event plane method.

where the average runs over all possible quadruplets of particles,(a, b, c, d), emitted in the collision, and over events. This can be generalized to an arbitrary even number of particles, which yields higher order estimates $v_n\{6\}$, $v_n\{8\}$, etc.

The second multiparticle method [138] was used to analyze directed flow v_1 in the STAR [105, 111] and NA49 [129] experiments. It relies on a study of *three*-particle correlations and involves both v_1 and v_2:

$$\left\langle e^{i(\phi_a+\phi_b-2\phi_c)} \right\rangle \simeq (v_1)^2 v_2 \ . \tag{3.11}$$

Normally, the elliptic flow, v_2, is obtained first using either two-particle ($v_n\{2\}$) or four-particle ($v_n\{4\}$) cumulant method. Then, the above equation can be used to obtain an estimate of v_1, which is denoted by $v_1\{3\}$ since it involves a three-particle correlation.

The practical implementation of the cumulant method in real experiments is more difficult, as the detectors do not have full azimuthal coverage. To get correct results for the flow components, extra terms, such as acceptance correction factors, resolution parameters and weighting (similar to that of the event plane method) must be added in order to remove inaccuracies arising from detector inefficiencies, and the number of these terms increases tremendously as the order of the cumulant increases [129]. At the same time, the statistical errors also increase.

On the other hand, in order to apply the four-particle correlation approach –which is claimed to give the most reliable estimates of the elliptic flow [129]– to the analysis of real data, one should perform an average over all possible quadruplets of particles in a given event. Bearing in mind that the average multiplicity in collisions at RHIC energies is well beyond a thousand, it becomes a non-trivial task. The simplest solution to the problem is the *four-subevent* method [104], where the detected particles partitioned into four subevents and a flow vector for each of them is calculated, $Q_n = \sum_k u_{n,k}$, where the sum is over all particles in the subevent and $u_{n,k} = e^{in\phi_k}$. Thus, the problem becomes much simpler computationally:

$$-v_n^4 = \left\langle \frac{Q_{n,1}Q_{n,2}Q^*_{n,3}Q^*_{n,4}}{M_1M_2M_3M_4} \right\rangle - 2\left\langle \frac{Q_{n,1}Q^*_{n,2}}{M_1M_2} \right\rangle^2 \tag{3.12}$$

where M_i are the corresponding subevent multiplicities.

3.3.2 Possible problems with recent techniques

Some of the weak points of the introduced methods have already been pointed out above. In this section, we will focus on the possible problems connected to these techniques, which may lead to serious inaccuracy in the flow analysis and in final flow results.

In the *event plane method* the first problem arise already when the azimuth of the event plane, Ψ_n, is estimated via the event flow vector, Q_n, using equation (3.6). It is easy to see that each measurable harmonic can yield an independent estimated Ψ_n, thus, the event planes, which are estimates of the same reaction plane, may differ from one-another. The difference might be small, or might even be corrected when the resolution of the event plane is calculated, but – according to our knowledge – none of the experiments has reported results of such investigation, if any has been done.

Furthermore, the summation goes over the whole acceptance of the detector, which is symmetric in rapidity, y, [104]. Without proper weighting taking into account the sign of rapidity, the *first harmonic*, v_1, is eliminated by construction, because it involves a forward-backward azimuthal antisymmetry, and so, the forward and backward contributions may cancel each other. The importance of weighting was actually pointed out in the original paper, which described the method for finding the event plane [87], but in some experimental papers discussing flow analysis it was not clearly stated whether such weighting had been used. For instance, in one of the STAR papers [104] the definition of the event flow vector, Q_n (3.5), first appears *without* any weighting factors. This might be misleading. In the very recent paper [111] this lack was corrected, however, only in the latest version, six months after the first electronic publication. The results presented are not changed, and we do hope that the weighting was *indeed* applied in the calculations.

One might argue that such a forward-backward azimuthal anti-correlation is a consequence of momentum conservation, thus, it is a non-flow correlation, like the cumulant method treats it. However, fluid dynamics is nothing else but the collective form of energy and momentum conservation. More precisely, in the infinite particle number limit, fluid dynamics really leads to a single particle momentum distribution after integrating the contributions of all fluid elements. This is a consequence of the assumption of local equilibrium, a fundamental assumption in fluid dynamics, and the assumption of molecular chaos. When we consider *finite multiplicities* and smaller samples, correlations may arise from global momentum conservation. To subtract these correlations as non-flow effects is questionable. Moreover, at the end of the collision, fluid dynamics must be supplemented by some freeze out prescription to obtain measurables. Since in the freeze out process local thermal equilibrium ceases to exist, the post FO distribution must be an out of equilibrium, non-thermal distribution. In the FO process the assumption of molecular chaos does not hold, so the FO process leads to correlations. There is a third effect, inherent in fluid dynamical descriptions when *sudden and rapid hadronization* coincides with the freeze out. This can be described in a non-thermal string fragmentation, coalescence or recombination picture,

which might lead to correlations also. The above mentioned three effects fundamentally influence the measured flow patterns, and it is highly questionable if these should be excluded from the flow analysis, as it is done in the cumulant method.

The proper determination of higher *odd harmonics* can be similarly problematic. The lack of information provided by the longitudinal motion of emitted particles and the longitudinal symmetries and asymmetries severely impair the analysis of the collective flow. Therefore, the identification of the reaction plane is essential, although, as we pointed out earlier, it is a non-trivial task and it might be a source of inaccuracy when it appears *directly* in the flow calculations via the azimuth of estimated event plane, Φ_n. Still, the reaction plane should be determined, even if one analyzes flow components using the cumulant method, where the azimuth of the reaction plane does not show up in the calculations directly. Moreover, besides the azimuth of the reaction plane, one should also determine the direction of the impact parameter vector $\vec{b}$. It is a weakness of the cumulant method that it eliminates the information about the reaction plane.

In case of *even harmonics* exclusively, the weighting and the identification of reaction plane does not seem to be too important and one may conclude (wrongly) that it can be omitted without severe consequences. For even harmonics, there is a symmetry for positive and negative x-values, and so, the projectile-target directions cannot be identified, i.e. only the reaction plane is identified but not the direction of the impact parameter vector $\vec{b}$. If this estimated reaction plane is used for the evaluation of the coefficients, v_n, the target and projectile directions will appear randomized in the sample.

If weighting is used, but it is forward-backward symmetric, e.g. $w_i(y) = v_2(y)$ [104], this does not solve the problem discussed here. As a consequence, forward-backward azimuthal asymmetries will be eliminated by this misidentification even if they exist. We will show examples to explain and demonstrate this in section 3.4.2.

Due to complicated experimental setups, the event plane determination and flow analysis vary to a large extent, and the different methods are even mixed with each other. In these cases it is very difficult to judge the accuracy and precision of the flow analysis. Examples are the most recent evaluation of directed flow, v_1, by the STAR collaboration [111, 142], where the three-cumulant method [138] was combined with the event plane method [87], and the four-subevent method [104] described above in section 3.3.1.

3.3.3 Experimental results on v_n

At the Relativistic Heavy Ion Collider (RHIC), three of the four experiments – PHENIX, PHOBOS and STAR– study anisotropic flow. Since RHIC began

operation in 2000, these experiments have produced a wealth of information on the flow components [101–115]. PHOBOS and PHENIX have mostly studied elliptic flow and reported only preliminary results on directed flow, so far. In all their analysis the *event plane method* was used [106–110, 114, 115]. STAR has performed more extensive studies of collective flow with a great variety of the applied methods.

In these section, we will show some of the experimental results in order to illustrate our concerns related to the possible problems of the experimental techniques.

Directed flow at RHIC

Let us start with the study of directed flow, which is clearly the most problematic flow component, however, a very important one because of the possible appearance of the "wiggle" structure, which might be directly related to quark-gluon plasma formation, as described in section 3.2.2.

Among the RHIC experiments, directed flow was studied only in STAR. The first v_1 analysis [105] was done using the *three-particle cumulant method* [138]. The result is shown in figure 3.4, on the right hand side. In the pseudorapidity region $|\eta| < 1.2$, $v_1(\eta)$ is approximately flat with a slope of $(-0.25 \pm 0.27(stat))\%$ per unit of pseudorapidity, which is in principle consistent with theoretical predictions [95, 130]. However, due to the large statistical error bars it can neither be confirmed nor invalidated that a "wiggle" shows up. The pseudorapidity dependence of v_1 in the projectile fragmentation region is very similar to that observed at full SPS energy.

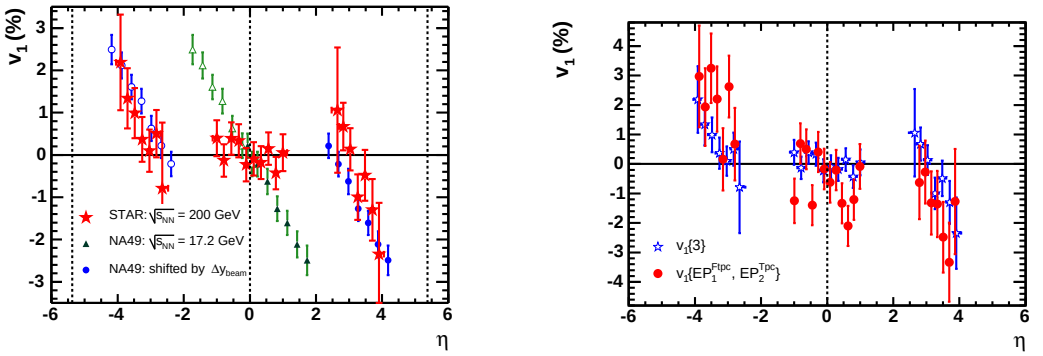

Figure 3.4: Directed flow of charged hadrons as a function of pseudorapidity at STAR [105, 111]. Left: The values of $v_1\{3\}$ [105] (stars) for centrality 10–70%. Right: The values of $v_1\{\mathrm{EP}_1, \mathrm{EP}_2\}$ [111] (circles) for centrality 20–60%.

In the most recent paper [111], directed flow analysis was performed with a somewhat different method, which combined the three-particle cumulant

method [138] with the event plane method [87]. This technique was first used by Oldenburg [142] based on the experimental setup. First, one determines two first order event planes $\Psi_1^{\mathrm{FTPC_1}}$ and $\Psi_1^{\mathrm{FTPC_2}}$ in the two Forward Time Projection Chambers (one for each), and the second order event plane Ψ_2^{TPC} in the main Time Projection Chamber, applying the event plane method [87]. Then, the directed flow is calculated in the same manner as it was described in the three-cumulant method by equation (3.11), correlating the particles with the first and second order event planes, EP_1 and EP_2, represented by their azimuthal angles, Ψ_1^{FTPC} and Ψ_2^{TPC}, respectively, instead of correlation with two other particles. The usual notation for v_1 in this case is $v_1\{\mathrm{EP}_1, \mathrm{EP}_2\}$. Results from such an analysis is also presented in figure 3.4, on the right hand side. One can see that the statistical errors are even bigger than in the case of $v_1\{3\}$. In the mid-pseudorapidity region the slope is $v_1 = (-0.5 \pm 0.5(stat))\%y$, which agrees with the $v_1\{3\}$ result within error and the two results are even consistent with zero within error. Still, having statistical errors with the same magnitude as that of the results, one can not conclude that the slope is zero and there is no "wiggle", as it was claimed in [143]. The only conclusion which holds is that the measurement must be improved. It is also questionable that the directed flow is *really* so small around midrapidity. As we have pointed out in section 3.3.2, improper weighting using the cumulant method may eliminate the directed flow by construction. Unfortunately, a pure event plane method can not be performed, because the first harmonic event plane is poorly defined in the TPC due to the inefficient experimental setup. It was stated nine months ago [144] that a new detector was going to be built into the present setup to increase the accuracy of the reaction plane identification. Unluckily, results are not yet available, if this improvement was already done. We have also found it rather surprising that in the very recent, one hundred pages long summary paper of the STAR Collaboration [113], which reviews the most important experimental results of nucleus-nucleus collision studies at STAR during the operation of RHIC so far, the term *directed flow* or v_1 is not even mentioned, neither as a predicted signature of QGP nor as a measured observable. Study of directed flow is either not listed in the section which describes the short- or longer-term goals of the experiment. Nevertheless, the elliptic flow is well discussed.

Elliptic flow at RHIC

The analysis of elliptic flow and higher even harmonics of the Fourier expansion is far less baffling than that of odd harmonics. The use of different techniques of flow analysis does not lead to huge differences in the results.

As it is expected, the cumulant method yields somewhat smaller elliptic

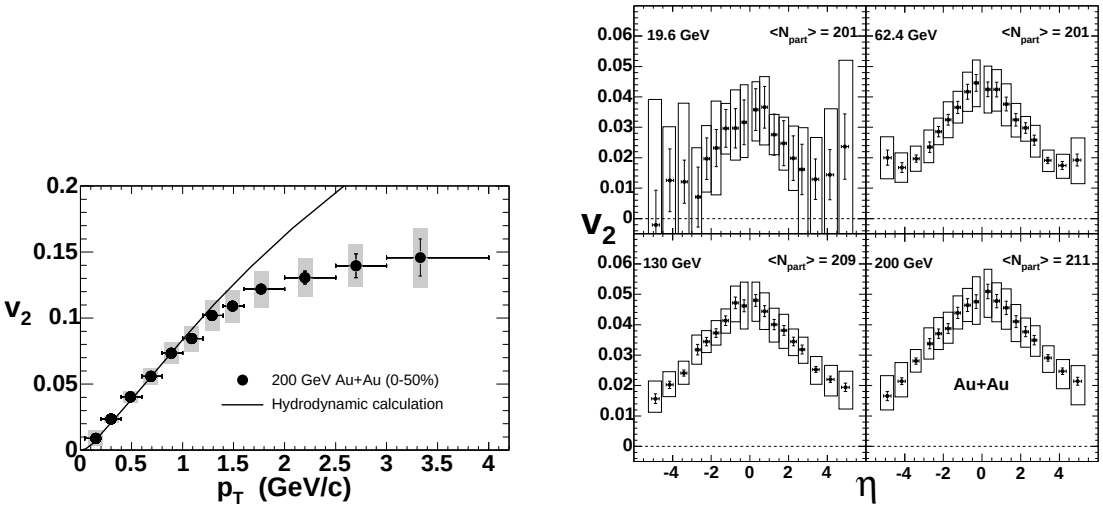

Figure 3.5: Elliptic flow of charged particles at PHOBOS [115]. Left: Elliptic flow as a function of transverse momentum for particles emitted near midrapidity ($0 < \eta < 1.5$) in Au+Au collisions at $\sqrt{s_{NN}} = 200$ GeV. Grey boxes show the systematic uncertainties of the data. Right: Pseudorapidity dependence of elliptic flow for the most central collisions (40%) of Au-Au at a variety of beam energies. Note the linear fall-off at higher $|\eta|$ and the lack of evidence for a constant value over a broad midrapidity region. Boxes indicate systematic uncertainties.

flow components than the event plane method because of the elimination of non-flow (and maybe also some flow) effects, but does not change the qualitative properties of flow results dramatically.

Elliptic flow studies in three RHIC experiments have resulted in numerous publications [101–115]. Here we will show some of the most recent results just to give an impression of the gained information.

The PHOBOS Collaboration recently reviewed the dependence of elliptic flow on transverse momentum and pseudorapidity for charged particles [115]. The results are presented in figure 3.5. In PHOBOS, the flow analysis was performed using the event plane method. The results show that elliptic flow is large at RHIC energies. Over a wide range of centrality and transverse momentum, the value near midrapidity is as large as that calculated under the assumption that a boost-invariant relativistic hydrodynamic fluid was formed. However, no boost-invariant central plateau is seen in the $v_2(\eta)$ plot. Recently, STAR also has produced results on the pseudorapidity dependence of v_2 at 15–20% centrality [111] and indications of a central plateau appears there.

The STAR Collaboration reported results of higher even harmonics, such as v_4, and v_6, as well. These are presented in figure 3.6 As a function of p_t, v_4 rises more slowly from the origin than v_2, but does flatten out at high p_t like

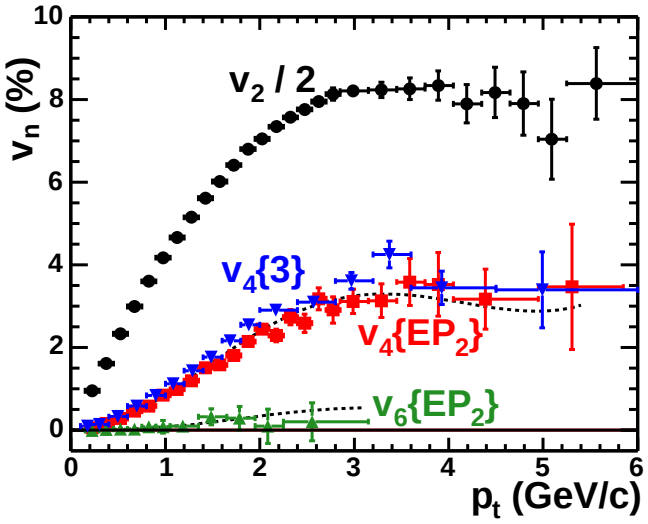

Figure 3.6: The values of v_2, v_4, and v_6 with respect to the second harmonic event plane as a function of transverse momentum, p_t, for $|\eta| < 1.2$ [105]. The v_2 values have been divided by a factor of two to fit on scale. The three particle cumulant values (triangles) for v_4 ($v_4\{3\}$) are also shown. The dashed curves are $1.2 \cdot v_2^2$ and $1.2 \cdot v_2^3$.

v_2. The rise is almost linear in both cases up to $p_t \approx 2\,\mathrm{GeV}$. The $v_6(p_t)$ values are consistent with zero. Ollitrault has proposed for the higher harmonics that v_n might be proportional to $v_2^{n/2}$ [105]. In order to test the applicability of this scaling, v_2^2 and v_2^3 were also plotted in the figure as dashed lines. The proportionality constant has been taken to be 1.2 in order to fit the v_4 data.

3.4 Model calculation of flow components

As we discussed in section 3.2.1, flow analysis is an important issue of relativistic heavy ion collision studies, as it might provide us with valuable information on the early stages of the collision.

One of the main goals of this PhD project was to investigate the flow phenomena using the Multi Module Model. As the flow analysis involves the frozen out particles emerging from the collision, realistic flow calculations from the model can be done only if we have a complete freeze out description and a well identified freeze out surface. We have discussed the freeze out problem and our achievements in freeze out modeling in chapter 2. We have shown that freeze out modeling is a very complex and non-trivial task and we ran into numerous difficulties during the work. Unfortunately, the

freeze out module is still not ready, thus, we are not yet able to perform realistic flow analysis. However, the code for the numerical calculation of all flow components has been worked out in an independent module, which is completed and can be coupled to the previous modules when those are ready for use. We tested the code by applying it directly on a simple, blast wave type of hydrodynamical model, which we developed just for this aim following the scheme of the ellipsoidally symmetric Buda-Lund hydro model [145–148].

Thus, we have calculated directed and elliptic flow from a tilted, ellipsoidally expanding particle emitting source. The tilt angle, Θ, represents the rotation of the major (longitudinal) direction of expansion from the direction of the beam. We have performed calculations with several tilt angles and ellipsoids with different deformation.

We have divided our fireball into cubic cells by a grid in x, y, z coordinates, as it is done in most hydrodynamic models, also in the second module of our Multi Module Model. The aim of the introduced discretization was to produce similar output as those of the second (hydro) and third (freeze out) modules, which makes it possible to change the simple blast wave model to the more sophisticated Multi Module Model without further changes in the next steps of the calculation, when the latter is ready.

Also, the freeze out layer is discretized on this grid. Due to this discretization, the "fluid-cells" do not match the spherical layer exactly, the volume of the cells, and so all conserved quantities have some discretization error. This depends on the choice of radius, layer thickness, cell size and the way which cells are selected to be in the layer. However, one can vary these parameters to achieve a small relative error in the normalization. Our set of parameters yields a relative error somewhat below 1%, which is much smaller than the statistical errors of the experimental techniques.

Results of this flow analysis were presented on international conferences and published in international refereed journals [24, 149, 150]. Two of the papers can be found in appendix C.7 and C.8. Below we will repeat some of the results of these papers.

3.4.1 Theoretical background

The contribution of a fluid cell to the final baryon phase-space distribution is [42]:

$$\frac{dN_c}{d^3p} = \gamma\, V_{cell}\ \frac{p^\mu\, d\sigma_\mu}{p^0}\ \ f_{F.O.}(x,\, p)\ , \tag{3.13}$$

where $\gamma\, V_{cell}$ is the proper volume of a fluid cell, $f_{F.O.}(x,\, p)$ is the freeze out distribution and $d\sigma_\mu$ is the normal of the freeze out surface.
Using the relations $p = (p^0, p_\parallel, \vec{p}_\perp)$, $p_\parallel = p^0\ dy$ and $p_t = |\vec{p}_\perp|$, the azimuthal

distribution per unit rapidity takes the form

$$\frac{dN_c}{dy\ d\phi} = \int \frac{d^3p}{dy\ d\phi}\ \frac{dN_c}{d^3p} = \gamma\, V_{cell} \int \frac{d^3p}{dy\ d\phi}\ \frac{p^\mu\, d\sigma_\mu}{p^0}\ f_{F.O.}(x,\, p) =$$

$$= \gamma\, V_{cell} \int dp_t\ p_t\ \ (p^\mu\, d\sigma_\mu)\ f_{F.O.}(x,p) \equiv \int dp_t\ p_t\ G_c(p_t, \phi_{CM}, y)\ . \quad (3.14)$$

When we evaluate the azimuthal asymmetry, this is done with respect to the reaction plane. The ϕ_{CM} is the azimuth angle of particles in the center of mass (CM) frame, where these are measured. Then, the coefficients of the different harmonics, v_1, v_2, etc. can be evaluated via additional numerical integrations over ϕ_{CM} azimuth angle. Thus, the flow components can be expressed as

$$v_n(y) = \frac{\sum\limits_c \int \cos\left(n\phi_{CM}\right) \gamma\, V_{cell}\ (p^\mu\, d\sigma_\mu)\ f_{F.O.}(x,p) d^2p_t}{\sum\limits_c\ dN_c/dy}\ , \quad (3.15)$$

where the sums go over all fluid cells, c. Derivation of equation (3.15) can be found in appendix B in section B.2.

For the freeze out surface we may assume that the local momentum distribution is a Jüttner distribution :

$$f_{F.O.}(x,\, p) = f^{J\ddot{u}ttner}(p) \equiv \frac{g_n}{(2\pi\hbar)^3} exp\left(\frac{\mu - p^\mu u_\mu}{T}\right)\ .$$

In this case equation (3.15) takes the form

$$v_n(y) = \frac{\sum\limits_c K\, \gamma V_{cell} \int dp_t\ p_t\ d\phi_{CM}\ \cos\left(n\,\phi_{CM}\right) g_c(p_t, \phi_{CM}, y)}{\sum\limits_c\ dN_c/dy} \quad (3.16)$$

where the following notations were introduced:

$$g_c(p_t, \phi_{CM}, y) \equiv \left[H\,\sqrt{m^2 + p_\perp^2} - \ \vec{p}_\perp\, \gamma_\sigma\, \vec{d\sigma}_\perp\ \right] \cdot e^{-h\,\sqrt{m^2+p_\perp^2} + \vec{p}_\perp\,\vec{g}}\ ,$$

$$H \equiv \gamma_\sigma(\cosh y - d\sigma_{||}\ \sinh y)\ , \qquad h \equiv \gamma(\cosh y - v_{||}\ \sinh y)\ /\ T\ ,$$

$$\vec{g} \equiv \gamma\ \vec{v}_\perp\ /\ T\ , \quad K \equiv (g_n \cdot e^{\,\mu/\,T})/(2\pi\hbar)^3 = (g_n \cdot n)/(4\pi\, m^2\, T\, K_2(m/T))\ .$$

Derivation of equation (3.16) and further explanation of the introduced quantities are presented in appendix B.

To calculate the flow components, v_n, one has to perform double integrations. Unfortunately, the computation of the numerator can only be done numerically, even in the case of the simple Jüttner distribution. However, the denominator, which is actually the rapidity distribution of particles, dN/dy, has an analytical solution. The solution for the case when the flow four-vector, u^μ, is parallel to the normal of the surface, $d\sigma^\mu = u^\mu$, was derived and shown in Csernai's text book [42] in chapter 7. For the more realistic general case of $d\sigma^\mu \neq u^\mu$, such analytical result, according to our knowledge, has not been shown yet in the literature. We have, however, found an analytic solution in this latter case as well, and derived a relatively simple formula to calculate the rapidity distribution, i.e. the denominator of the v_n harmonics:

$$\frac{dN_c}{dy} = 2\pi\, K\, \gamma V_{cell}\, \gamma \prime^3\, \frac{H}{h} m^2 \left(1 - \frac{g\,G}{h\,H}\right) \left[\frac{2\,\gamma \prime^2}{h^2\, m^2} + \frac{2\,\gamma \prime}{h\, m} + 1\right] e^{-\frac{h}{\gamma \prime} m} \ . \quad (3.17)$$

Equation (3.17) describes the contribution of one fluid cell to the final rapidity distribution, dN/dy, which can be calculated by summing over all fluid cells, i.e. $dN/dy = \sum_c dN_c/dy$. Details of the derivation are shown in appendix B. The new formula makes further calculations faster, because we can reduce the number of time consuming numerical integrations.

However, equation (3.17) is valid *only* if the post FO distribution is Jüttner type. We have discussed it in chapter 2 that the post FO distribution can not be a thermal one, thus, neither a Jüttner distribution. Nevertheless, in the test of our code we have assumed that $f_{F.O.} = f^{Jüttner}$, which was computationally more effective, but the code is written in a way that the post FO distribution can be easily changed to a more realistic one, such as cut Jüttner or canceling Jüttner etc.

3.4.2 Results for directed and elliptic flow

In this section we *summarize* the main results from our model calculations. For more details please consult the papers in appendices C.7 and C.8. We would like to emphasize that the primary aim of these evaluations was not to reproduce the experimental data –although this will be an important task in the future to check our Multi Module Model–, but to test the flow module on a simpler collision model. Furthermore, we had another important goal, namely to demonstrate why the identification of the reaction plane is so important, and how the odd harmonics may be eliminated by construction using the cumulant method without proper weighting. We have discussed the above problems in section 3.3.2. As we have mentioned there, the acceptance of the detector is symmetric in rapidity [104]. Odd harmonics involve a forward-backward azimuthal antisymmetry, therefore, without weighting by

rapidity taking into account the sign of it, i.e. whether the detected particle came from the target or projectile side, the forward and backward contributions may cancel each other. This problem may be negligible only if the emitting source is not tilted. For even harmonics there is a forward-backward symmetry, thus the role of introducing weights with opposite signs for positive and negative rapidities in the event plane or cumulant method is not transparent. To show this, we have calculated flow components from two tilted ellipsoidally expanding sources, which differ from one-another *only* in the sign of the tilt angle,Θ, which illustrates the situation where the projectile and target sides are changed. Then we calculated the average of both the directed and elliptic flow components coming from the two oppositely tilted sources, which simulates the case when only the reaction plane is identified, but not the impact parameter, as the projectile and target directions are not known.

We have first investigated the rapidity, y, dependence of the directed flow, v_1, and elliptic flow, v_2. Figures are shown in papers C.7 and C.8. The results for $v_2(y)$ obtained from the two oppositely tilted ellipsoids are nearly identical, which confirms our predictions. This may lead to the wrong conclusion that weighting is not important. In paper C.7 we presented results of elliptic flow as a function of the transverse momentum, $v_2(p_t)$, as well. This result is actually less relevant for our primary aim, but demonstrates that even a simple blast wave model can reproduce some of the main characteristics of the observed data. We calculated $v_2(p_t)$ only for a small p_t region, because it was shown earlier [101] that elliptic flow at RHIC can be described by hydrodynamical models only for p_t up to 2 GeV/c. Our $v_2(p_t)$ rises almost linearly up to $p_t = 1\,\mathrm{GeV/c}$, then deviates from a linear rise and starts to saturate.

The results for the directed flow are more interesting. First of all, $v_1(y)$ is definitely not constant zero at midrapidities and the "wiggle" structure appears. The situation changes dramatically when we construct the "averaged" v_1, which demonstrates what happens when we partly reverse the projectile and target side. In this case $v_1(y)$ is in principle set to zero, $v_1(y) \approx 0$.[5]

We have also investigated the dependence of flow pattern on the initial geometry of the fireball by calculating flow components from two ellipsoidal sources with the same thermodynamical properties but different geometries, i.e. with different ratio of the three half axes. Such investigation might have an importance in understanding the initial stages of heavy ion collisions. As the development of flow is related to the conditions in the nuclear matter

[5]The discretization to finite fluid cells leads to some inaccuracy in our calculations around mid-rapidity for small ($|\Theta| < 10°$) tilt angles, which are absent with bigger angles, but theoretical considerations do not support that the source can be more tilted at RHIC energies.

formed in the collision, the measured flow might provide us with information also on the initial geometry if we know how the geometry effects the flow. Of course, with such an oversimplified model as the one we used, one can not expect quantitative conclusions. However, our results support the expectations derived from pure phenomenology that a highly deformed and tilted source develops stronger flow.

So far we have not calculated higher harmonics, but those calculations are straightforward using our model and equation (3.15). It will make more sense to study higher harmonics with the Multi Module Model.

Chapter 4

Conclusions

Reaction modeling is presently a bottleneck in research advance. In the field of ultra-relativistic heavy ion physics the reaction mechanism is extremely complicated and difficult to model. It was suggested that a realistic model should consist of several *modules*, in which the different stages of the reaction are each described by suitable theoretical approaches. The construction of such a model, the so-called *Multi Module Model* [12], was started a few years ago. The goal of this PhD project was to develop the already existing, but far not complete Multi Module Model, specially focusing on the last module which describes the final stages of a heavy ion collision, as this module was still missing. The major original achievements summarized in this thesis correspond to the freeze out problem and calculation of an important measurable, the anisotropic flow.

4.1 Summary of results

Freeze out

The importance of freeze out models is that they allow the evaluation of observables, which then can be compared to the experimental results. Therefore, it is crucial to find a realistic freeze out description, which is proved to be a non-trivial task. Recently, several kinetic freeze out models have been developed. Based on the earlier results, we have introduced new ideas and improved models, which may contribute to a more realistic description of the freeze out process.

We have investigated the applicability of the Boltzmann Transport Equation (BTE) to describe dynamical freeze out. We have pointed out that the BTE approach has some basic limitations in the FO description, since some of the standard assumptions, which are used to derive the BTE from the conservation laws in a space-time domain, can not be fulfilled in a freeze out

process.

To overcome this problem, we have introduced the so-called *Modified Boltzmann Transport Equation*, which has a form very similar to that of the BTE, but takes into account those characteristics of the FO process which the BTE can not handle, e.g. the rapid change of the phase-space distribution function in the direction normal to the finite FO layer.

We have shown that the main features of earlier ad hoc kinetic FO models can be obtained from BTE and MBTE. We have discussed the qualitative differences between the two approaches and presented some quantitative comparison as well (appendices C.1, C.2 and C.3).

Since the introduced modification of the BTE makes it very difficult to solve the FO problem from the first principles, it is important to work out simplified phenomenological models, which can explain the basic features of the FO process. We have built and discussed such a model.

Our model is based on earlier kinetic FO models, but still unique, since we have generalized the kinetic freeze out treatment for *finite* time-like and space-like FO layers, and the model can handle both time-like and space-like freeze out processes on the same fully covariant footing (appendices C.4 and C.5).

Flow analysis

The other main subject of this thesis has been the collective flow in heavy ion collisions. Collective flow from ultra-relativistic heavy ion reactions is an important hadronic observable sensitive to the early stages of system evolution.

The flow analysis involves the particles, which have already been frozen out. Therefore, to perform realistic flow computations from the Multi Module Model we need a complete freeze out description and a well identified freeze out surface. However, the freeze out module is still not ready. Although we have not yet been able to evaluate collective flow using the Multi Module Model, the method and code for the calculation of flow components has been worked out in an independent module. This module is completed and can be coupled to the previous modules when those are ready for use.

In order to test the code, we have calculated directed and elliptic flow from a tilted, ellipsoidally expanding source using a simple, blast wave type of model. This model was developed directly for this aim based on Buda-Lund hydro models.

We also pointed out some possible problems connected to the experimental techniques used for calculation of the v_n flow components, which may lead to serious inaccuracy in the experimental flow analysis. We have demonstrated our concerns using the results from the above model.

Although, this oversimplified blast wave model is not suitable to reproduce the experimental data –which will be an important task in the future to check our Multi Module Model–, it has provided us with important information. We have found that the directed flow, v_1, is very sensitive to the correct identification of the reaction plane included the determination of the impact parameter *vector*, and can be misinterpreted by some experimental methods. We have shown that misidentification of the reaction plane may even set the directed flow to zero by construction.

We have presented results of the rapidity dependence of the directed flow, v_1, and elliptic flow, v_2, furthermore, the transverse momentum dependence of v_2. We have also investigated the dependence of the flow pattern on the initial geometry of the fireball by calculating flow components from two ellipsoidal sources with the same thermodynamical properties but different shape.

Our papers focusing on the collective flow are included in appendices C.6, C.7 and C.8.

4.2 Outlook

As we pointed out in section 2.5, the code determining the freeze out hypersurface should still be improved in order to avoid inaccuracies in the further calculations. We have to find a reliable method how to exclude the space-time clusters arising from temperature fluctuations, caused by late negative pressure of the supercooled QGP in the fluid dynamical model. So far it was done by stopping the time evolution of the surface at a given time. It can, however, lead to exclusion of fluid elements, which should be taken into account.

When the freeze out hypersurface is reliably determined, the measurables can be evaluated, based on the identified surface. For this aim we have to find the post FO distribution. Conservation laws on the FOHS can be satisfied using the relativistic Rankine-Hugoniot or Taub relations [39, 40] if the post FO state is in local thermodynamical equilibrium. Unfortunately, kinetic FO models indicate that the post FO matter is *never* in local equilibrium, so for accurate results, conservation laws have to be evaluated based on the actual post FO matter properties. The use of a Jüttner phase space distribution is just a first approximation. This has to be modified to avoid negative contributions by introducing a "cut" [41], like in section 2.2.2. The real, calculated post FO distribution is even more complicated but, as we have shown in section 2.2, some analytic approximations do exist.

Measurables could be evaluated using a set of simplified approximate solutions for the post FO distribution, such as Jüttner, cut Jüttner and canceling Jüttner distributions. Then, comparing the different model results

to each other and to the experimental data, one could investigate the level of inaccuracy in different levels of approximation.

Regarding the flow analysis, further work should include the study of energy dependence of flow components for different hadronic species, which could give information on pressure and pressure gradients in the nuclear matter created in the collision. Investigation of impact parameter dependence is also necessary.

Due to its structure, where different stages of the reaction are described in different modules, the Multi Module Model is highly suitable for execution on a GRID. The simulation of heavy ion reactions is a repeated task for several impact parameters, beam energies, etc. This makes it possible for the different modules of our model to be executed simultaneously, and GRID computing is probably the fastest and most effective way to perform these computational task.

A future aim can be the development of the necessary software to make the Multi Module Model applicable for GRID computing.

Bibliography

[1] J. C. Collins and M. J. Perry, *Phys. Rev. Lett.* **34** (1975) 1353 ;
G. Baym and S. A. Chin, *Phys. Lett.* **B 88** (1976) 241;
B. A. Freedman and L. D. McLerran, *Phys. Rev.* **D 16** (1977) 1196;
G. Chapline and Nauenberg, *Phys. Rev.* **D 16** (1977) 450;
E. V. Shuryak, *Phys. Lett.* **B 78** (1978) 150;
O. K. Kalashnikov and V. V. Klimov, *Phys. Lett.* **B 88** (1979) 328;
J. I. Kapusta, *Nucl. Phys.* **B 148** (1979) 461.

[2] U. Heinz and M. Jacob, (nucl-th/0002042) CERN Press Release 2000.
http://pressold.web.cern.ch/PressOld/Releases00/PR01.00EQuarkGluonMatter.html

[3] H. Satz, *Nucl. Phys.* **A 715** (2003) 3.

[4] N. K. Glendenning, *Compact Stars, Nuclear Physics, Particle Physics, and General Relativity*, (Springer-Verlag, New York, 2000).

[5] Ágnes Nyíri, *Quark-Gluon Plasma in Neutron Stars*, M.Phil. Thesis in Physics, UiB (2001).
`http://www.ift.uib.no/~nyiri/master_thesis.ps`

[6] Á. Nyíri, *J. Phys.* **G 28** (2002) 2073.

[7] F. Karsch *et al.*, *Phys. Lett.* **B 478** (2000) 447;
F. Karsch, *Nucl. Phys.* **A 698** (2002) 199.

[8] F. Csikor *et al.*, hep-lat/0301027.

[9] BRAHMS homepage: http://www4.rcf.bnl.gov/brahms/WWW/;
PHENIX homepage: http://www.phenix.bnl.gov/;
PHOBOS homepage: http://www.phobos.bnl.gov/;
STAR homepage: http://www.star.bnl.gov/.

[10] J. D. Bjorken, *Phys. Rev.* **D 27** (1983) 140.

[11] Csaba Anderlik, *Hadronization and Freeze-out in Heavy Ion Collisions*, Dr.Scient Thesis in Physics, UiB (2001).

[12] Volodymyr K. Magas, *Multi Module Model for Ultra-Relativistic Heavy Ion Collisions*, Dr.Scient Thesis in Physics, UiB (2001).

[13] Cs. Anderlik, Z.I. Lázár, V.K. Magas, L.P. Csernai, H. Stöcker and W. Greiner, *Phys. Rev.* **C 59** (1999) 388 (nucl-th/9808024).

[14] Cs. Anderlik, L.P. Csernai, F. Grassi, W. Greiner Y. Hama, T. Kodama, Zs. Lázár, V. Magas and H. Stöcker, *Phys. Rev.* **C 59** (1999) 3309 (nucl-th/9806004).

[15] V.K. Magas, Cs. Anderlik, L.P. Csernai, F. Grassi, W. Greiner Y. Hama, T. Kodama, Zs. Lázár and H. Stöcker, *Heavy Ion Phys.* **9** (1999) 193 (nucl-th/9903045).

[16] V.K. Magas, Cs. Anderlik, L.P. Csernai, F. Grassi, W. Greiner Y. Hama, T. Kodama, Zs. Lázár and H. Stöcker, *Phys. Lett.* **B 459** (1999) 33 (nucl-th/9905054).

[17] V.K. Magas, Cs. Anderlik, L.P. Csernai, F. Grassi, W. Greiner Y. Hama, T. Kodama, Zs. Lázár and H. Stöcker, *Nucl. Phys.* **A 661** (1999) 596c (nucl-th/0001049).

[18] V.K. Magas, L.P. Csernai and D.D. Strottman, *Phys. Rev.* **C 64** (2001), 014901 (hep-ph/0010307).

[19] L.P. Csernai, D. Röhrich, V.K. Magas and Cs. Anderlik, *Proceedings of the "RHIC 2000"*, Shadow Ridge Resort, Park City, Utah, USA, March 11-18, 2000 - http://theo08.nscl.msu.edu/RHIC2k/proceedings.htm

[20] F.H. Harlow, *Proc. Symp. Appl. Math.* **15** (1963) 269; A.A. Amsden, Los Alamos Scientific Laboratory Report, LA-3466 (1966).

[21] F.H. Harlow, A.A. Amsden and J.R. Nix, *J. Comp. Phys.* **20** (1976) 119.

[22] A.K. Holme, E.F. Staubo, L.P. Csernai, E. Osnes and D. Strottman, *Phys.Rev.* **D 40** (1989) 3735;
E.F. Staubo, A.K. Holme, L.P. Csernai, M. Gong and D. Strottman, *Phys. Lett.* **B 229** (1989) 351;
E.F. Staubo, L.P. Csernai, A.K. Holme and D. Strottman, *Phys. Scripta* **T 32** (1990) 190;
N.S. Amelin, E.F. Staubo, L.P. Csernai, V.D. Toneev, K.K. Gudima and D. Strottman, *Phys. Lett.* **B 261** (1991) 352; *Phys. Rev. Lett.* **67** (1991) 1523;
N.S. Amelin, L.P. Csernai, E.F. Staubo and D. Strottman, *Nucl. Phys.*

A 544 (1992) 463;
L.V. Bravina, L.P. Csernai, P. Lévai, N.S. Amelin and D. Strottman, *Nucl. Phys.* **A 566** (1994) 461;
L.V. Bravina, L.P. Csernai, P. Lévai and D. Strottman, *Phys. Rev.* **C 50** (1994) 2161.

[23] *Modeling of Boltzmann Transport Equation for Freeze Out*
K. Tamosiunas, L.P. Csernai, V.K. Magas, E. Molnár, Á. Nyíri, *J. Phys.* **G 31** (2005) 1001.

[24] *Hydrodynamics: Overview*
L.P. Csernai, E. Molnár, Á. Nyíri and K. Tamosiunas, *J. Phys.* **G 31** (2005) 951.

[25] *Phase Transitions in High Energy Heavy Ion Collisions*
L.P. Csernai, A. Anderlik, Cs. Anderlik, A. Keranen, V.K. Magas, J. Manninen, E. Molnár, Á. Nyíri, B.R. Schlei, D.D.Strottman and K. Tamosiunas, Proceedings of NATO ASI on *Structure and Dynamics of Elementary Matter* (2004) p. 127, ISBN 1-4020-2445-2, edited by W. Greiner, M.G. Itkis, J. Reinhardt and M. Cem Guclu, (hep-ph/0401005).

[26] *Multi Module Modeling of Heavy Ion Reactions and the 3rd Flow Component*
L.P. Csernai, A. Anderlik, Cs. Anderlik, V.K. Magas, E. Molnár, Á. Nyíri, D. Röhrich and K. Tamosiunas, *AIP Conference Proceedings* Vol. 739 (2004) p. 330, ISBN 0 7354 0223 X, Edited by E. Ferreira and T. Kodama, (hep-ph/0408183).

[27] *Canceling Jüttner Distributions for Space-like Freeze Out*
K. Tamosiunas, L.P. Csernai, J. Manninen, E. Molnár and Á. Nyíri, *AIP Conference Proceedings* Vol. 739 (2004) p. 652, ISBN 0 7354 0223 X, Edited by E. Ferreira and T. Kodama

[28] L.D. Landau, *Izv. Akad. Nauk SSSR* **17** (1953) 51.

[29] F. Cooper and G. Frye, *Phys. Rev.* **D 10** (1974) 186.

[30] L.P. Csernai, Zs. Lázár and D. Molnár, *Heavy Ion Phys.* **5** (1997) 467.

[31] Yu.M. Sinyukov, S.V. Akkelin, Y. Hama, *Phys. Rev. Lett.* **89** (2002) 052301 (nucl-th/0201015);
S.V. Akkelin, M.S. Borysova, Yu.M. Sinyukov, *Acta Phys.Hung.* **A 22** (2005) 165 (nucl-th/0403079).

[32] L.V. Bravina, I. N. Mishustin, N.S. Amelin, J.P. Bondorf and L.P. Csernai, *Phys. Lett.* **B 354** (1995) 196.

[33] V.K. Magas, A. Anderlik, Cs. Anderlik and L.P. Csernai, *Eur. Phys. J.* **C 30** (2003) 255.

[34] E. Molnár, L.P. Csernai, V.K. Magas, Á. Nyíri and K. Tamosiunas, Submitted to *Phys. Rev.* **C**, (hep-ph/0503047).

[35] E. Molnár, L.P. Csernai, V.K. Magas, Zs.I. Lázár, Á. Nyíri and K. Tamosiunas, Submitted to *Phys. Rev.* **C**, (hep-ph/0503048).

[36] V.K. Magas, L.P. Csernai, E. Molnár, Á. Nyíri and K. Tamosiunas *Nucl. Phys.* **A 749** (2005) 202, (hep-ph/0502185).

[37] L.P. Csernai, V.K. Magas, E. Molnár, Á. Nyíri and K. Tamosiunas, *Eur. Phys. J.* **A 25** (2005) 65, (hep-ph/0505228).

[38] L.P. Csernai, V.K. Magas, E. Molnár, Á. Nyíri and K. Tamosiunas, to be submitted to *Phys. Rev.* **C** *Rap. Comm.* (revised version of hep-ph/0406082).

[39] A.H. Taub, *Phys. Rev.* **74** (1948) 328.

[40] L.P. Csernai, *Sov. JETP* **65** (1987) 216; *Zh. Eksp. Theor. Fiz.* **92** (1987) 379.

[41] K.A. Bugaev, *Nucl. Phys.* **A 606** (1996) 559.

[42] L. P. Csernai, *Introduction To Relativistic Heavy Ion Collisions*, Wiley (1994)

[43] L.V. Bravina, I.N. Mishustin, N.S. Amelin, J.P. Bondorf and L.P. Csernai, *Phys. Lett.* **B 354** (1995) 196.

[44] L.V. Bravina, I.N. Mishustin, J.P. Bondorf and L.P. Csernai, *Heavy Ion Phys.* **5** (1997) 455.

[45] F. Grassi, Y. Hama and T. Kodama, *Phys. Lett.* **B 355** (1995) 9.

[46] F. Grassi, Y. Hama and T. Kodama, *Z. Phys.* **C 73** (1996) 153.

[47] F. Grassi, Y. Hama, T. Kodama and O. Socolowski, *Heavy Ion Phys.* **5** (1997) 417.

[48] H. Heiselberg, *Heavy Ion Phys.* **5** (1997) 435.

[49] T. Csörgő and L.P. Csernai, *Phys. Lett.* **B 333** (1994) 494.

[50] L.P. Csernai and I.N. Mishustin, *Phys. Rev. Lett.* **74** (1995) 5005.

[51] L.P. Csernai and M. Gong, *Phys. Rev.* **D 37** (1988) 3231.

[52] M. Gyulassy and L.P. Csernai, *Nucl. Phys.* **A 460** (1986) 723.

[53] F. Jüttner, *Ann. Phys und Chemie,* **34** (1911) 856.
I. Abonyi, *Acta Phys. Hung.* **23** (1967) 247.

[54] K.A. Bugaev and M.I. Gorenstein, *arXiv:* nucl-th/9903072.

[55] K. Tamosiunas and L. P. Csernai, Eur. Phys. J. **A 20** (2004) 269 (hep-ph/0403179).

[56] K.A. Bugaev, *Phys. Rev. Lett.* **90** (2003) 252301.

[57] K.A. Bugaev, *Phys. Rev.* **C 70** (2004) 034903 (nucl-th/0401060).

[58] D. Molnar and M. Gyulassy, *Phys. Rev.* **C 62** (2000) 054907 (nucl-th/0005051).

[59] J.J. Neumann, B. Lavrenchuk and G. Fai, *Heavy Ion Phys.* **5** (1997) 27.

[60] J. Sollfrank, *J. Phys.* **G 23** (1997) 1903.

[61] D.H. Rischke, *Nucl. Phys.* **A 698** (2002) 153 (nucl-th/0104071).

[62] N. Ardex, F. Grassi, Y. Hama and O. Socolowski, *arXiv:* nucl-th/0102056.

[63] Y.B. Ivanov, V.N. Russkikh and V.D. Toneev, nucl-th/0503088.

[64] A. Keranen, L.P. Csernai, V. Magas and J. Manninen, *Phys. Rev.* **C 67** (2003) 034905.

[65] B.R. Schlei, FOHS movie – `http://www.ift.uib.no/~nyiri/b500T139.mov`

[66] U. Heinz, *Nucl. Phys.* **A 638** (1998) 357c.

[67] R. Stock, *Nucl. Phys. Lett.* **456** (1999) 277.

[68] J. Stachel, *Nucl. Phys.* **A 654** (1999) 119c.

[69] U. Heinz, *Nucl. Phys.* **A 685** (2001) 414c.

[70] M. Becattini *et al.*, *Eur. Phys. J.* **C 5** (1998) 143.

[71] S. Jeon and V. Koch, Phys. *Rev. Lett.* **85** (2000) 2076.

[72] M. M. Aggarwal *et al.* (WA98 Collaboration), *Phys. Rev. Lett.* **93** (2004) 022301 (nucl-ex/0310022);
M. M. Aggarwal *et al.* (WA98 Collaboration), *Phys. Rev. Lett.* **85** (2000) 3595 (nucl-ex/0006008);
M. M. Aggarwal *et al.* (WA98 Collaboration), *Phys. Rev. Lett.* **83** (1999) 926 (nucl-ex/9901009).

[73] J. Frantz *et. al.* (PHENIX Collaboration), *J. Phys.* **G 30** (2004) 1003.

[74] X.-N. Wang and M. Gyulassy, *Phys. Rev.* **D 44** (1991) 3501.

[75] X. N. Wang, *Phys. Rev.* **C 63** (2001) 054902.

[76] Y. L. Dokshitzer and D. E. Kharzeev, *Phys. Lett.* **B 519** (2001) 199.

[77] I. Arsene *et. al.*, *Phys. Rev. Lett.* **91** (2003) 072305.

[78] J. Adams *et. al.*, *Phys. Rev. Lett.* **91** (2003) 072304.

[79] W.Scheid, H. Müller and W. Greiner, *Phys. Rev. Lett.* **32** (1974) 741.

[80] G. F. Chapline, M. H. Johnson, E. Teller and M. S. Weiss, *Phys. Rev.* **D 8** (1973) 4302.

[81] H. A. Gustafsson *et al.*, (Plastic Ball Coll.), *Phys. Rev. Lett.* **53** (1984) 544.

[82] P. Danielewicz and G. Odyniecz, *Phys. Lett.* **B 157** (1985) 146.

[83] W. Reisdorf and H.G. Ritter, *Annu. Rev. Nucl. Part. Sci.* **47** (1997) 663;
N. Herrmann, J.P. Wessels, and T. Wienold, *Annu. Rev. Nucl. Part. Sci.* **49** (1999) 581.

[84] J. Y. Ollitrault, *Phys. Rev. D* **46** (1992) 229;
J. Y. Ollitrault, *Phys. Rev. D* **48** (1993) 1132.

[85] H.H. Gutbrod, K.H. Kampert, B. Kolb, A.M. Poskanzer, H.G. Ritter, R. Schicker and H.R. Schmidt (Plastic Ball Collaboration) , *Phys. Rev.* **C 42** (1990) 640.

[86] S. Voloshin and Y. Zhang, *Z. Phys.***C 70**, (1996) 665.

[87] A. M. Poskanzer and S. A. Voloshin, *Phys. Rev.* **C 58** (1998) 1671.

[88] L. Bravina, L.P. Csernai, P. Lévai, and D. Strottman, *Phys. Rev.* **C 50**, (1994) 2161;
L. Bravina, *Phys. Lett.* **B 344**, (1995) 49 .

[89] C.M. Hung and E.V. Shuryak, *Phys. Rev. Lett.* **75**, (1995) 4003.

[90] J. Stachel, *Nucl. Phys.* **A 610** (1996) 509;
B.A. Li, C.M. Ko, *Phys. Rev.* **C 52**, (1995) 2037;
53, R22 (1996);
B.A. Li, C.M. Ko, G.Q. Li, *Phys. Rev.* **C 54**, (1996) 844.

[91] D.H. Rischke, *Nucl. Phys.* **A 610**, (1996) 88.

[92] P. Danielewicz, *Phys. Rev.* **C 51**, (1995) 716;
P. Danielewicz, R.A. Lacey, P.-B. Gossiaux, C. Pinkenburg, P. Chung, J.M. Alexander, and R.L. McGrath, *Phys.Rev.Lett.* **81** (1998) 2438 (nucl-th/9803047).

[93] B. Zhang, M. Gyulassy and C. M. Ko, *Phys. Lett.* **B 455** (1999) 45.

[94] D. Teaney and E.V. Shuryak, *Phys. Rev. Lett.* **83** (1999) 4951;
D. Teaney, J. Lauret and E.V. Shuryak, *Phys. Rev. Lett.* **86** (2001) 4783.

[95] L.P. Csernai and D. Röhrich, *Phys. Lett.* **B 458** (1999) 454 (nucl-th/9908034).

[96] J. Brachmann *et al.*, *Phys. Rev. C* **61** (2000) 024909.

[97] M. Bleicher and H. Stöcker, *Phys. Lett.* **B 526** (2002) 309.

[98] RIKEN BNL Research Center Proceedings, vol. 62: *New Discoveries at RHIC – The Strongly Interacting Quark-Gluon Plasma*, BNL-72391-2004 (2004).

[99] M. Gyulassy and L. McLerran, *Nucl. Phys.* **A 750** (2005) 30 (nucl-th/0405013).

[100] H. Sorge, *Phys. Rev. Lett.* **78** (1997) 2309;
H. Sorge, *Phys. Lett.* **B 402** (1997) 251;
H. Sorge, *Phys. Rev. Lett.* **82** (1999) 2048.

[101] C. Adler *et al.*, (STAR Coll.), *Phys. Rev. Lett.* **90** (2003) 032301 (nucl-ex/0206006).

[102] J. Adams *et al.*, (STAR Coll.), *Phys. Rev. Lett.* **93** (2004) 252301 (nucl-ex/0407007).

[103] C. Adler *et al.*, (STAR Coll.), *Phys. Rev. Lett.* **87** (2001) 182301 (nucl-ex/0107003).

[104] C. Adler *et al.*, (STAR Coll.), *Phys. Rev.* **C 66** (2002) 034904 (nucl-ex/0206001).

[105] J. Adams *et al.*, (STAR Coll.), *Phys. Rev. Lett.* **92** (2004) 062301 (nucl-ex/0310029).

[106] B. B. Back *et al.*, (PHOBOS Coll.), *Phys. Rev. Lett.* **89** (2002) 222301.

[107] S. Manly *et al.*, (PHOBOS Coll.), *Nucl. Phys.* **A 715** (2003) 611.

[108] B. B. Back *et al.*, (PHOBOS Coll.), *Phys. Rev. Lett.* **94** (2005) 122303.

[109] K. Adcox *et al.*, (PHENIX Coll.), *Phys. Rev. Lett.* **89** (2002) 212301 (nucl-ex/0204005).

[110] S. S. Adler *et al.*, (PHENIX Coll.), *Phys. Rev. Lett.* **91** (2003) 182301 (nucl-ex/0305013).

[111] J. Adams *et al.*, (STAR Coll.), *arXiv:* nucl-ex/0409033 v3.

[112] J. Adams *et al.*, (STAR Coll.), *arXiv:* nucl-ex/0504022.

[113] J. Adams *et al.*, (STAR Coll.), *Nucl. Phys.* **A 757** (2005) 102 (nucl-ex/0501009).

[114] K. Adcox *et al.*, (PHENIX Coll.), *Nucl. Phys.* **A 757** (2005) 184 (nucl-ex/0410003).

[115] B. B. Back *et al.*, (PHOBOS Coll.), *Nucl. Phys.* **A 757** (2005) 28 (nucl-ex/0410022).

[116] A. K. Holme, E. F. Staubo, L.P. Csernai, E. Osnes and D. Strottman, *Phys. Rev.* **D 40** (1989) 3735.

[117] D.H. Rischke, Y. Pürsün, J.A. Maruhn, H. Stöcker and W. Greiner, *Heavy Ion Phys.* **1** (1995) 309.

[118] C.M. Hung and E.V. Shuryak, *Phys. Rev. Lett.* **75** (1995) 4003.

[119] N. S. Amelin, E.F. Staubo, L.P. Csernai, V.D. Toneev, K.K. Gudima and D.D. Strottman, *Phys. Rev. Lett.* **67** (1991) 1523.

[120] L. Bravina, L.P. Csernai, P. Lévai and D. Strottman, *Phys. Rev.* **C 50** (1994) 2161.

[121] J. Brachmann, A. Dumitru, J.A. Maruhn, H. Stöcker, W. Greiner and D. Rischke, *Nucl. Phys.* **A 619** (1997) 391.

[122] J. Barette *et al.*, (E814 Collaboration) *Phys. Rev. Lett.* **73** (1994) 2532; J. Barette *et al.*, (E814 Collaboration) *Phys. Lett.* **B 351** (1995) 93.

[123] N.N. Ajitanand *et al.* (E895 Collaboration), *Nucl. Phys.* **A 638** (1997) 415.

[124] L. Ahle *et al.* (E802 Collaboration), *Phys. Rev.* **C 57**, (1998) 1416.

[125] J. Barrette *et al.* (E877 Collaboration), *Phys. Rev. Lett.* **70**, (1993) 2996;
J. Barrette *et al.* (E877 Collaboration), *Phys. Rev.* **C 55**, (1997) 1420;
J. Barrette *et al.* (E877 Collaboration), *Phys. Rev.* **C 56**, (1997) 3254;
J. Barrette *et al.* (E877 Collaboration), *Nucl.Phys.* **A 661** (1999) 329;
J. Barrette *et al.* (E877 Collaboration), *Phys.Rev.* **C 59** (1999) 884;
J. Barrette *et al.* (E877 Collaboration), *Phys.Lett.* **B 485** (2000) 319;
J. Barrette *et al.* (E877 Collaboration), *Phys.Rev.* **C 63** (2001) 014902.

[126] H. Appelshäuser *et al.* (NA49 Collaboration), *Nucl. Phys.* **A 638** (1998) 463;
H. Appelshäuser *et al.* (NA49 Collaboration), *Phys. Rev. Lett.* **80** (1998) 4136;
A. M. Poskanzer *et al.* (NA49 Collaboration), *Nucl. Phys.* **A 661** (1999) 341 (nucl-ex/9906013).

[127] M. M. Aggarwal *et al.* (WA98 Collaboration), *Eur. Phys. J.* **C 41** (2005) 287;
M. M. Aggarwal *et al.* (WA98 Collaboration), *Phys. Lett.* **B 469** (1999) 30;
M. M. Aggarwal *et al.* (WA98 Collaboration), *Nucl. Phys.* **A 638** (1998) 459 (nucl-ex/9807004).

[128] A. Wetzler *et al.*, NA49 Collaboration, *Nucl. Phys.* **A 715** (2003) 583 (nucl-ex/0212023).

[129] C. Alt *et al.*, NA49 Collaboration, *Phys. Rev.* **C 68** (2003) 034903 (nucl-ex/0303001).

[130] R.J.M. Snellings *et al.*, *Phys. Rev. Lett.* **84** (2000) 2803.

[131] D. Myers, *Nucl. Phys.* **A 296** (1978) 177.

[132] J. Gosset, J.I. Kapusta and G.D. Westfall, *Phys. Rev.* **C 18** (1978) 844.

[133] L.P. Csernai, A. Anderlik, Cs. Anderlik, V.K. Magas, E. Molnár, Á. Nyíri, D. Röhrich and K. Tamosiunas, *Acta Phys. Hung.* **A**, in press (2005) (hep-ph/0405277).

[134] S. Wang *et al.*, *Phys. Rev.* **C 44** (1991) 1091.

[135] P. Danielewicz, *Phys. Rev.* **C 51** (1995) 716.

[136] P. M. Dinh, N. Borghini and J.-Y. Ollitrault, *Phys. Lett.* **B 477** (2000) 51 (nucl-th/9912013).

[137] N. Borghini, P. M. Dinh and J.-Y. Ollitrault, *Phys. Rev.* **C 62** (2000) 034902 (nucl-th/0004026).

[138] N. Borghini, P. M. Dinh, J.-Y. Ollitrault, A.M. Poskanzer and S.A. Voloshin, *Phys. Rev.* **C 66** (2002) 014901 (nucl-th/0202013).

[139] N. Borghini, P. M. Dinh and J.-Y. Ollitrault, *Phys. Rev.* **C 63** (2001) 054906 (nucl-th/0007063).

[140] N. Borghini, P. M. Dinh and J.-Y. Ollitrault, *Phys. Rev.* **C 64** (2001) 054901 (nucl-th/0105040).

[141] N. Borghini, P. M. Dinh and J.-Y. Ollitrault, *Phys. Rev.* **C 66** (2002) 014905 (nucl-th/0204017).

[142] M. D. Oldenburg, Poster presented at "Quark Matter 2004" (nucl-ex/0403007).

[143] A.H. Tang (for the STAR Collaboration), *J. Phys.* **G 30** (2004) 1235 (nucl-ex/0403018).

[144] A.H. Tang (STAR Collaboration), private discussion on the "SQM 2004" Conference, 15-20 September, 2004.

[145] M. Csanád, T. Csörgő and B. Lörstad, *Nukleonika* **49** (2004) S45 (nucl-th/0402036).

[146] M. Csanád, T. Csörgő and B. Lörstad, *Nucl. Phys.* **A 742** (2004) 80 (nucl-th/0310040).

[147] T. Csörgő and B. Lörstad, *Phys. Rev.* **C 54** (1996) 1390 (hep-ph/9509213)

[148] T. Csörgő and B. Lörstad, *Nucl. Phys.* **A 590** (1995) 465 (hep-ph/9503494).

[149] Á. Nyíri and L.P. Csernai, *Acta Phys. Hung.* **A**, in press (2005)

[150] Á. Nyíri, L.P. Csernai, E. Molnár and K. Tamosiunas, *J. Phys.* **G 31** (2005) 1045.

[151] L.P. Csernai and D.D. Strottman, eds., *Relativistic Heavy Ion Physics*, Vol. 1,2, World Scientific (1991).

[152] L.D. Landau, E.M. Liftshits, *Course of Theoretical Physics*, Vol. 6, *Fluid mechanics*, Butterworth-Heinemann (1987).

[153] I. S. Gradstejn and I. M. Ryzhik, *Table of integrals, series and products*, New York: Academic Press (1965).